



저작자표시-비영리-변경금지 2.0 대한민국

이용자는 아래의 조건을 따르는 경우에 한하여 자유롭게

- 이 저작물을 복제, 배포, 전송, 전시, 공연 및 방송할 수 있습니다.

다음과 같은 조건을 따라야 합니다:



저작자표시. 귀하는 원저작자를 표시하여야 합니다.



비영리. 귀하는 이 저작물을 영리 목적으로 이용할 수 없습니다.



변경금지. 귀하는 이 저작물을 개작, 변형 또는 가공할 수 없습니다.

- 귀하는, 이 저작물의 재이용이나 배포의 경우, 이 저작물에 적용된 이용허락조건을 명확하게 나타내어야 합니다.
- 저작권자로부터 별도의 허가를 받으면 이러한 조건들은 적용되지 않습니다.

저작권법에 따른 이용자의 권리는 위의 내용에 의하여 영향을 받지 않습니다.

이것은 [이용허락규약\(Legal Code\)](#)을 이해하기 쉽게 요약한 것입니다.

[Disclaimer](#)

의학 박사 학위 논문

Novel strategies using montelukast to suppress fibrosis around
silicone implants

몬테루카스트를 통한 실리콘 보형물의 섬유화를 억제하는
새로운 전략

2018 년 8 월

서울대학교 대학원

의학과 의학 전공

김 병 휘

Novel strategies using montelukast to suppress fibrosis around
silicone implants

몬테루카스트를 통한 실리콘 보형물의 섬유화를 억제하는 새로운 전략

지도교수 최 영 빈

이 논문을 의학박사학위논문으로 제출함

2018 년 8 월

서울대학교 대학원

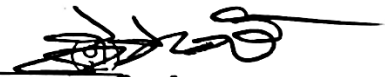
의학과 의공학 전공

김 병 휘

김병휘 의 박사학위논문을 인준함

2018 년 8 월

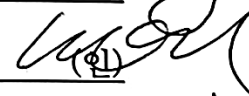
위 원 장 허 찬 영



부 위 원 장 최 영 빈

(인) 

위 원 고 원 건

(인) 

위 원 윤 형 진



위 원 이 정 찬



Abstract

Novel strategies using montelukast to suppress fibrosis around silicone implants

Byung Hwi Kim

Department of Medicine

The Graduate School

Seoul National University

Implantable silicon medical devices have evolved in various forms depending on their use. However, there are limitations to their use due to side effects that occur after *in vivo* transplantation. Among implantable silicone medical devices, many side effects have been reported in silicone breast implants. A typical side effect is the occurrence of capsular contracture, which is mediated by an *in vivo* immune response. In severe cases, capsular contracture may require secondary surgery and is associated with pain and abnormal breast shape. Thus, it is important to understand the side effects that may occur when inserting silicone breast implants and to identify potential measures to suppress the side effects associated with fibrosis.

In this study, I investigated the fibrogenesis associated with *in vivo* implants and inhibited fibrosis by controlling drug delivery. By analyzing the morphogenesis of macrophages, the overall process associated with the fibrosis–inhibition mechanism was verified. In addition, an implant with effective fibrosis–inhibiting properties was developed through the introduction of a new drug called montelukast, and its efficacy was verified. To verify the tissue factors involved in the fibrosis reaction steps, a shell of a silicone implant 2 cm in diameter was prepared. After drug loading, the shell was

bonded using a medical bonding agent so that the surface was exposed on both sides. Four different groups of samples (SI, PLGA_SI, MON_SI and PLGA_MON_SI) were prepared and implanted into a subcutaneous pocket in 8-week-old Sprague-Dawley rats. Biopsies were performed at five predetermined periods (1, 2, 4, 8, and 12 weeks) to verify suppression of the fibrosis pathway. Fibrosis- and inflammation-related factors, specifically, macrophages, fibroblasts, transforming growth factor- β (TGF- β), myofibroblasts, collagen density and capsule thickness were investigated. In the case of inflammatory factors, the expression pattern was high in the SI and PLGA_SI groups; however, the expression pattern in the MON_SI and PLGA_MON_SI groups after drug treatment was decreased in the early phase of the response to the foreign body. Fibrosis factors showed a tendency to increase continuously in the SI and PLGA_SI groups until week 12. Notably, in the MON_SI group, in which the drug was delivered for a short period of time (3 day drug release), the expression levels of fibrosis-related factors were low until week 4. However, the same results were observed in the group not receiving the drug (SI and PLGA_SI) at weeks 8 and 12 in the MON_SI group. In the PLGA_MON_SI group, all the fibrosis-related factors were suppressed for up to 12 weeks, and for the first time, it was verified that fibrosis could be suppressed by administration of the drug montelukast. Specifically, the number of macrophages in all the groups showed the same tendency, which was verified by differences in the macrophage phenotypes. In the PLGA_MON_SI group, the number of macrophages with the M1 phenotype was reduced early in the fibrosis pathway. On the other hand, the number of M2 phenotype macrophages was relatively high, thus suggesting that the stepwise nature of the immune response *in vivo* can be terminated early by montelukast.

Based on the above results, I demonstrated that montelukast may be applied to silicone implants and that it has an effective fibrosis suppressing function by controlling the fibrosis stage after placement of silicone implants. In addition, I demonstrated that early activation of macrophages with the M2 phenotype at the early stage of fibrosis induces early regulation of immune activity. Finally, the underlying mechanism of the fibrosis that occurs in response to silicone implants was determined,

and the results suggests the possibility that fibrosis can be suppressed by montelukast.

keywords: Capsular contracture, Fibrosis, Foreign body reaction, Macrophage phenotype,
Montelukast

Student Number: 2013-21721

Contents

List of Tables	ix
List of Figures	x
Chapter 1. Introduction	1
1.1 Research background.....	1
1.2 Capsular contracture.....	5
1.3 Montelukast and leukotrienes.....	8
1.4 Our research aims	10
Chapter 2. General theory of the fibrosis pathway response to silicone breast implants	11
2.1 The fibrosis processes.....	11
2.2 Methods for evaluation of fibrosis.....	14
2.2.1 Materials.....	14
2.2.2 Preparation of silicone implant samples	14
2.2.3 <i>In vivo</i> experimental procedures	16
2.2.4 Histological evaluation method.....	18
2.3 Overall information concerning fibrosis, cells and cellular factors.....	20
2.3.1 <i>In vivo</i> capsule thickness and collagen density.....	20
2.3.2 Inflammation analysis.....	23
2.3.3 Fibrosis-related factors	25
Chapter 3. Fibrosis suppression effect of montelukast in fibrosis pathway	29

3.1	Introduction	29
3.2	Materials and methods.....	33
3.2.1	Materials.....	33
3.2.2	Preparation of silicone implant samples	33
3.2.3	Sample characterization	36
3.2.4	<i>In vitro</i> drug release study	36
3.2.5	<i>In vivo</i> experiment.....	36
3.2.6	Histological and IF evaluation	38
3.2.7	Measurement of tissue tension	39
3.2.8	Statistical analysis.....	41
3.3	Results.....	42
3.3.1	Implant characterization.....	42
3.3.2	Capsule.....	45
3.3.3	Collagen.....	47
3.3.4	Inflammatory cells.....	49
3.3.5	Fibroblast.....	51
3.3.6	TGF- β	53
3.3.7	Macrophages	55
3.3.8	Myofibroblasts	57
3.3.9	Tissue tension	59
3.4	Discussion	62

3.5	Conclusion	65
Chapter 4. Analysis of macrophage phenotype changes induced by montelukast in the fibrosis pathway.....		
		66
4.1	Introduction	66
4.2	Materials and methods.....	68
4.2.1	Materials.....	68
4.2.2	Histological evaluation.....	68
4.3	Results.....	69
4.3.1	Number of M1 and M2 macrophages	69
4.3.2	M1 and M2 macrophage ratio analysis	72
4.4	Discussion	75
4.5	Conclusion	76
Chapter 5. Conclusion and Perspectives		
		77
References.....		
		82
Abstract in Korean		
		91

List of Tables

Table 3.1 Tensile force at failure of tissue	61
Table 4.1 M1/M2 ratio analysis	74

List of Figures

Figure 1.1 Information about Plastic surgery	4
Figure 1.2 Capsular contracture process <i>in vivo</i>	6
Figure 1.3 Hypothesis of fibrosis mechanism.....	7
Figure 2.1 Optical images of two groups silicone implant.....	13
Figure 2.2 Evaluation of capsule thickness and collagen density around the implants.....	18
Figure 2.3 Evaluation of inflammation score around the implants.....	20
Figure 2.4 Evaluation of TGF- β score.	22
Figure 2.5 Evaluation of fibroblast cell amount.	23
Figure 2.6 Evaluation of myofibroblast cell amoun	24
Figure 3.1 Schematic illustration of the preparation of the silicone implant samples.	31
Figure 3.2 Surgical procedure for implant insertion in live rats.	35
Figure 3.3 Representative image of the tissue biopsied from around the implant and used to measure tensile strength.....	37
Figure 3.4 Scanning electron micrographs of the surfaces, FTIR spectra and <i>In vitro</i> drug release profiles.....	40
Figure 3.5 Evaluation of capsule thickness around the implants	42
Figure 3.6 Evaluation of collagen density around the implants	44
Figure 3.7 Evaluation of the number of inflammatory cells (PMNs) around the implants	46
Figure 3.8 Evaluation of the number of fibroblasts around the implants.	48
Figure 3.9 Evaluation of the level of TGF- β expression around the implants	50
Figure 3.10 Evaluation of the number of macrophages around the implants.....	52
Figure 3.11 Evaluation of the number of myofibroblasts around the implants.	54

Figure 3.12 Tensile force at failure	56
Figure 4.1 Number of whole macrophages	66
Figure 4.2 Number of M1 and M2 macrophage	67
Figure 4.3 M1/M2 ratio graph.....	69

Chapter 1

Introduction

1.1 Research background

In the current era, the incidence of breast cancer is increasing every year, and it occurs frequently enough to be considered the second most frequent female cancer. Breast cancer is caused by genetic alterations (e.g., the HER2 gene) and lifestyle habits, and cases of severe breast cancer are commonly treated by removal of the whole breast. However, this treatment method forces women to give up their breasts, which may cause psychological problems, such as the loss of their sense of female sexuality [1, 2]. To resolve this issue, various surgical techniques have been developed to reconstruct a removed breast. Examples include autologous fat transplantation and placement of silicone breast implants [3, 4]. In general, when performing a mastectomy, it is difficult to obtain a sufficient volume of breast tissue through fat transplantation because the amount of fat that can be obtained from a patient is limited [3]. Therefore, it is common to perform breast reconstruction using a silicone breast implant. Silicone breast implants continue to be increasingly used in accordance with the increasing

interest in cosmetic surgery worldwide as well as with the increase in breast cancer. According to statistics reported by the Plastic Surgery Society, breast surgeries are the most frequently performed cosmetic surgeries around the world (Fig. 1.1). With the increasing trend in breast reconstruction and breast augmentation, the interest in breast implants continues to increase, thus increasing the occurrence of the side effects associated with breast implants.

Silicone breast implants are made of a silicone material that is composed of a round-shaped silicone shell filled with saline or silicone [5, 6]. Modern silicone breast implants were first introduced in 1963 and were smooth in nature. The second generation of breast implants developed had a thinner silicone shell with an emphasis on breast texture and natural breast shape. However, due to physical weakening of the shell, the implants tended to rupture. Due to these problems, the inner fill material of the breast implants was gradually modified to possess a sticky property to prevent leaking from the breast silicone implant site, and the thickness of the outer shell was gradually increased. Additionally, double lumen-shaped implants and polyurethane-based implants have also been developed to suppress the fatal side effect of capsular contracture, but this modification has gradually disappeared because of the continued occurrence of side effects, such as breast cancer and *in vivo* rupture. To prevent capsular contracture, a textured surface that mimics the outer shape of the polyurethane material has been developed and used. Furthermore, implants with a droplet shape and a microtextured surface are now commercially available. However, these silicone breast implants do not prevent the occurrence of side effects, and fibrosis and capsular contracture still occur. Capsular contracture is caused by excessive fibrosis induced by an immune response to the presence of foreign materials *in vivo* [7, 8]. This occurs in 9 ~ 11 % of patients with silicone breast implants and is the most frequently occurring side effect of silicone breast implants. Despite the improvements in the various forms of silicone breast implants (surface modification, minimization of physical stimulation, etc.), the occurrence of capsular contracture is still being reported. In recent years, research efforts have been directed toward ensuring *in vivo* safety by making the surface of the implants more uniform

or by chemically coating the surface to avoid immune reactions [9]. However, these developments have not yet been actualized, and to prevent capsular contracture (inhibition of fibrosis), oral administration with anti-fibrosis drugs (i.e., tranilast and zafirlukast) has been recommended. However, this approach has the disadvantage of long-term administration of a drug as well as additional side effects, such as secondary organ toxicity [10].

2017 TOP FIVE COSMETIC SURGICAL PROCEDURES

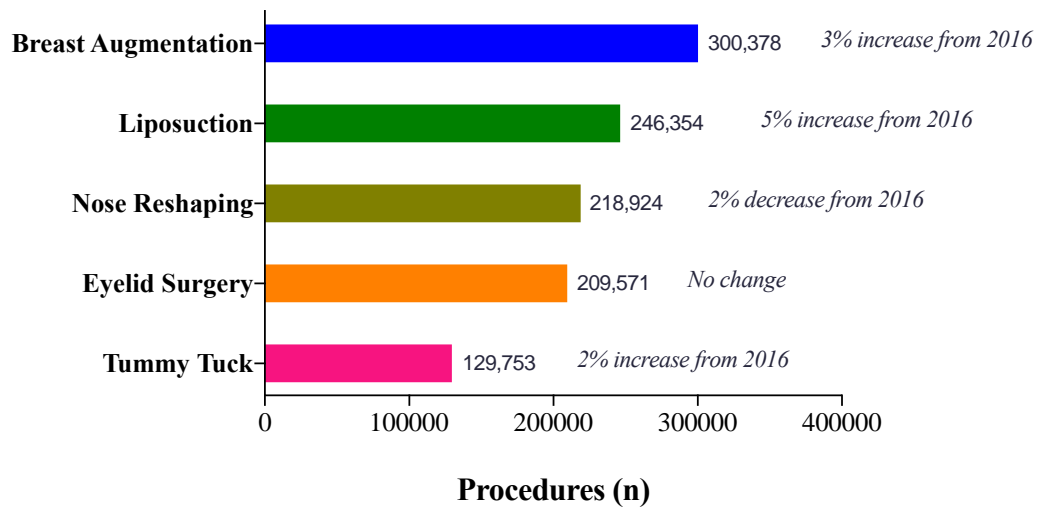


Figure 1.1 Information regarding plastic surgeries (American plastic surgery society, 2017)

1.2 Capsular contracture

Capsular contracture is a fatal side effect caused by fibrosis that is mediated by the immune response and proceeds via stepwise reactions involving various cellular factors (e.g., cytokines, the interleukin family, and $\text{TNF-}\alpha$) [2]. During the initial phase, platelets at the implantation site are stimulated by the wound, thereby initiating an early inflammatory response. In this process, $\text{TNF-}\alpha$ and members of the interleukin family (i.e., pre-inflammatory cytokines; IL-1 and IL-6), known as inflammatory mediators, are released by platelets and inflammatory cells, thus amplifying the early inflammatory response [11]. During this process, polymorphonuclear cells (PMNs; neutrophils, basophils, and eosinophils), known as inflammatory cells, are recruited to the implantation site, and the early inflammatory response is continued while the release of inflammatory factors continues. This inflammatory reaction begins immediately after implantation. The early inflammatory reaction is terminated within 3 days, and fibroblast and myofibroblast cell activation occurs in the late inflammatory reaction. Macrophages are the main factor involved in the progression from the early stage to the late inflammatory reaction, which is activated by inflammatory factors and increases via an autocrine effect [12]. These inflammatory cells are known to be PMNs and macrophages, which are activated by the immune response to a silicone breast implant and the release of various cytokines into the peripheral site of the silicone breast implant. Typically, $\text{TGF-}\beta$ is involved. Macrophages activated by specific factors then activate fibroblasts and myofibroblasts, the main cells participating in the late inflammatory response, by releasing $\text{TGF-}\beta$ again [13, 14]. These activated fibroblasts and myofibroblasts synthesize collagen around the implant, which forms a capsule on the periphery of the silicone breast implant, a reaction intended to isolate the foreign material. This reaction is called fibrosis, and in severe cases, it can cause capsular contracture. Capsular contracture causes the patient to suffer from pain, and a secondary surgery for removal of the silicone breast implant may be

necessary [15].

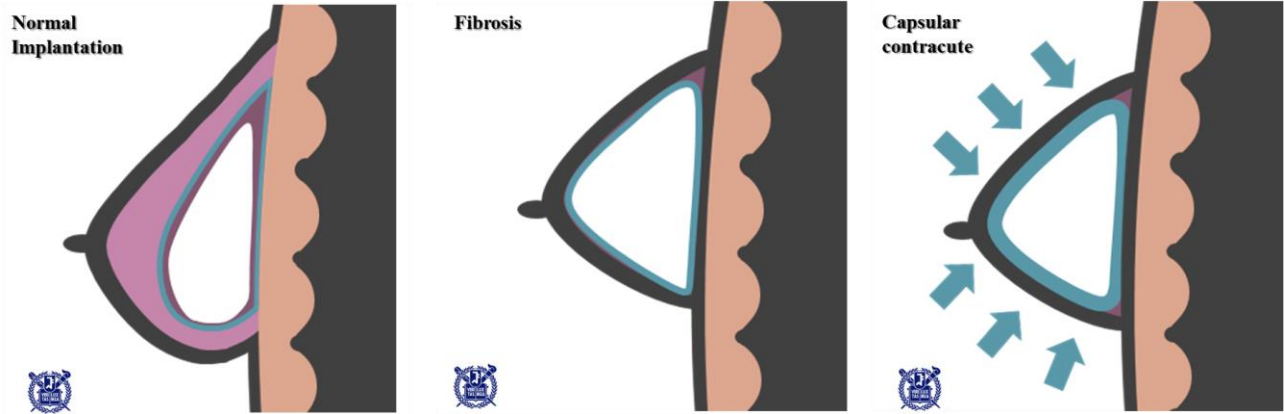


Figure 1.2 The capsular contracture process *in vivo*

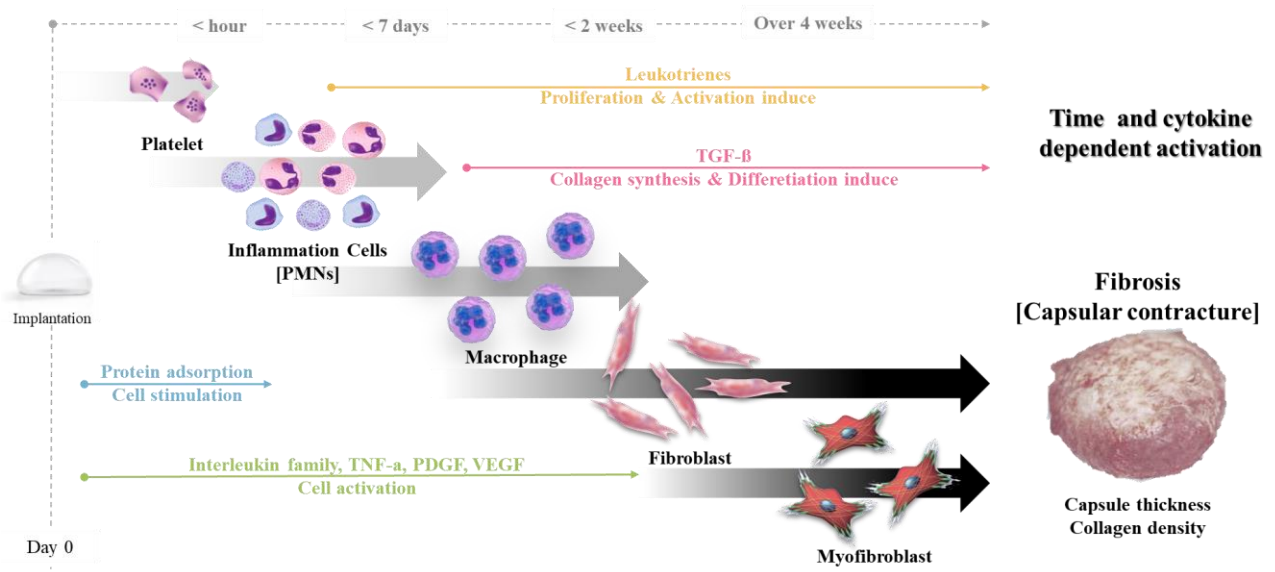


Figure 1.3 Hypothesis of the fibrosis mechanism

1.3 Montelukast and leukotrienes

Montelukast is a compound that selectively binds to the cysteinyl leukotriene receptor antagonist (LTRA) and is commonly used for asthma and acute inflammatory allergies [16]. Montelukast competitively binds to leukotriene receptors and decreases the activity of cells that have a leukotriene receptor on their membrane (i.e., PMNs, macrophages, fibroblasts, myofibroblasts and mast cells). In addition, montelukast decreases leukotriene production. In general, there are two types of leukotrienes: cysteinyl leukotrienes (CysLTs; leukotrienes C4, D4 and E4), which are a combination of cysteine leukotriene and leukotriene. Leukotriene B₄ binds to the leukotriene receptor to induce cell chemotaxis. CysLTs bind to cysteinyl leukotriene receptors _{1,2} (CysLTR₁ and CysLTR₂), resulting in bronchoconstriction, increased vascular permeability, inflammation, and hypersensitivity reactions [17]. These CysLTs are present on the cell membrane of a large number of cells that exhibit degranulation phenomena, including eosinophils and mast cells, and they are also present on macrophages and fibroblasts, which play a major role in the inflammatory response. Montelukast inhibits asthma by binding to these cells and inhibiting cellular activity or inhibiting the release of leukotrienes from these cells [18–20].

Leukotriene is a metabolite of the enzymatic activity of 5-lipoxygenase (5-LO) on arachidonic acid and has been identified as a potent inflammatory agent. Leukotrienes are synthesized in mast cells, eosinophils, neutrophils, monocytes, macrophages, and basophils and are also known to be synthesized in fibroblasts. There are a total of five types of leukotrienes, separated by two pathways involving arachidonic acid precursors (eicosanoids) [21]. Via the action of the enzymes COX-1 and 2, eicosanoids are converted to prostaglandins, but eicosanoids are converted to leukotrienes by 5-LO. Leukotrienes are converted to cysteinyl leukotrienes (C, D, E) and leukotriene B from leukotriene A. Among them, CysLTs play a role in maintaining inflammatory reactions. CysLTs

selectively bind to the CysLTR₁ and CysLTR₂, which are G protein-coupled receptors present on the cell surface, to increase cell activity and increase cell infiltration of PMNs [17]. Through increased PMN recruitment, the immune response is maintained inflammation in the tissue increases. This increased inflammation maintains and amplifies the *in vivo* immune response and leads to fibrosis via the activity and proliferation of late fibroblasts [22, 23].

1.4 Our research aims

The use of silicone breast implants is expected to continue to increase in the future, and the associated side effects are a major obstacle for patients who undergo breast reconstruction and breast augmentation surgeries. Thus, techniques to minimize these side effects will continue to evolve. To develop future implantable medical devices, the problem of fibrosis associated with *in vivo* implantation must be solved. To solve this problem, information concerning fibrosis-related factors must be collected, and research is needed to identify (through screening) more efficient drugs to suppress the side effects and to replace the existing anti-fibrosis techniques.

First, in Chapter 2, I aim to confirm the possibility of regulation of cellular activation and the major expression patterns in the fibrosis process following *in vivo* implantation. Additionally, I aim to examine the mechanisms of fibrosis development and obtain information regarding the fibrosis process. In addition, in Chapter 2, I try to verify the stages of fibrosis.

In Chapter 3, I try to verify the possibility of inhibiting fibrosis by introducing a new drug based on the information regarding the fibrosis process described in Chapter 2. In this regard, I apply the drug montelukast, which is currently used only as a conventional asthma medicine, to a silicone breast implant sample. To verify inhibition of leukotriene activity by montelukast, I analyzed the entire fibrosis process and the activity of fibrosis-related cells *in vivo*. In addition, I try to verify the different inhibitory effects reported in previous studies.

Finally, in Chapter 4, I attempt to further investigate differences in the expression patterns of macrophages and to evaluate whether any differences in the phenotype of these macrophages are present and, based on these results, to examine the mechanism by which the drug inhibits fibrosis.

Chapter 2

General theory of the fibrosis pathway response to silicone breast implants

2.1 The fibrosis processes

Fibrosis is an immune response that occurs *in vivo* and is caused by prolonged and sequential expression of cellular factors (e.g., interleukins, TNF- α and leukotrienes) [8]. Generally, fibrosis reactions are reported to occur due to implantation of medical devices or autoimmune reactions and are most frequently associated with breast implants [24]. Fibrosis reactions are initiated and changed according to the expression pattern of cellular factors *in vivo*. Finally, the fibrosis reaction terminates with the formation of a fibrous capsule around the implant. To avoid fibrosis, follow up screening of patients is performed for approximately 2 years to test for the occurrence of fibrosis [5, 25]. The fibrosis reaction is caused by chain reactions and the passage of time [26, 27], and therefore, fibrosis inhibition requires a clear analysis and effective regulation of the fibrosis mechanism.

Fibrosis occurs as a chain reaction and can be divided into six steps: 1. Blood–biomaterials

interaction; 2. Provisional matrix formation; 3. Acute inflammation; 4. Chronic inflammation; 5. Foreign body reaction; 6. Fibrous capsule formation [28, 29]. In the early stage, in the blood–biomaterial interaction phase, blood protein adsorption occurs due to leakage of blood during surgery, and in this step, the recruitment and activation of early inflammatory cells (PMNs) occurs due to the blood–derived proteins. In the second step, the recruited inflammatory cells (PMNs) and proteins form a matrix (provisional matrix) at the periphery of the implant containing active factors, and this matrix triggers the expression of early inflammatory cells [30, 31]. In the inflammatory reaction, the activation of PMNs and the expression of various cellular factors are predominantly stimulated via autocrine and paracrine effects. In this process, pro–inflammatory cytokines are predominantly expressed, and leukotriene is expressed [20]. Expression of these factors plays a major role in the next step of the cell activation reaction, and leukotriene affects the activity of cells (i.e., macrophages, fibroblasts and myofibroblasts) that are related to the fibrotic reaction throughout the entire fibrosis period [32, 33]. Inflammation reactions are divided into two phases: acute and chronic inflammation phases. Initially, during the acute inflammation phase, PMNs are predominantly present around the implant, and pro–inflammatory cytokines (i.e., IL–6, IL–10, IFN– γ and TNF– α) are secreted from these cells [34, 35]. In the late phase of fibrosis (chronic inflammation and foreign body reaction phase), the number of macrophages increases, leading to recruitment of fibroblasts. The expression of key factors associated with collagen synthesis, such as TGF– β , is increased by macrophages and fibroblasts. TGF– β expression causes a foreign body reaction (FBR), resulting in the formation of a foreign body giant cell (FBGC) through macrophage fusion. In addition, the number of fibroblasts necessary for the FBR response is greatly increased. Fibroblasts continuously proliferate and differentiate into myofibroblasts in response to TGF– β stimulation [36, 37]. The cells thus formed synthesize collagen, a fibrous capsule forms around the implant, and the immune response is terminated through isolation of the implant over time [7, 27].

Fibrosis does not cause any discomfort to the patient when it is properly terminated, but in

severe cases, it leads to capsular contracture, which causes pain and may require a secondary surgery. Capsular contracture is generally caused by various factors, such as excessive inflammation or overactivation of fibroblasts in the late phase of fibrosis. In this chapter, I confirm the degree of fibrosis over time and perform a stepwise analysis of the fibrosis that occurs when a silicone implant is placed based on knowledge of the overall fibrosis process.

2.2 Methods for evaluation of fibrosis

2.2.1 Materials

The clinical silicone shells were supplied by Hans Biomed (Seoul, Korea). EPO-TEK[®] 301-2 medical epoxy was obtained from Epoxy Technology (Billerica, MA, USA). For *in vivo* experiments, isoflurane was purchased from Hana Pharm (Seoul, Korea) and Bayer (Leverkusen, Germany). Paraformaldehyde (4 %) was supplied by KCFC (Korea). For staining, xylene, ethanol, an ammonia solution (28 %-30 %), acetic acid (1 %) and hydrochloric acid (35 %-37 %) were purchased from Duksan Pure Chemicals (Ansan, Korea). Modified Mayer's hematoxylin and eosin (H&E) Y solutions were supplied by Richard-Allan Scientific (MI, USA). Biebrich scarlet-acid fuchsin, phosphomolybdic acid, phosphotungstic acid and aniline blue solutions were purchased from Sigma-Aldrich (St. Louis, MO, USA). Target-retrieval solution (10×) and antigen diluent solution were obtained from Dako (Glostrup, Denmark). For immunofluorescence staining, anti-vimentin (ab92547), anti-TGF- β (ab92486) and anti- α -SMA (ab5694) antibodies were purchased from Abcam (Cambridge, MA, USA). Anti-CD163 antibody (MCA342R) was obtained from Biorad (Hercules, CA, USA).

2.2.2 Preparation of silicone implant samples

For implantation, I separately prepared two major silicone implant surface types (Fig. 2.1). In total, two groups of silicone implants were prepared for the *in vivo* evaluations, circular flat implants with either a textured or a smooth surface. The implant groups were prepared using only the silicone shell, which was cut into circles with a 2-cm diameter (1 mm thickness). Before implantation, all experimental samples were sterilized with ethylene oxide.

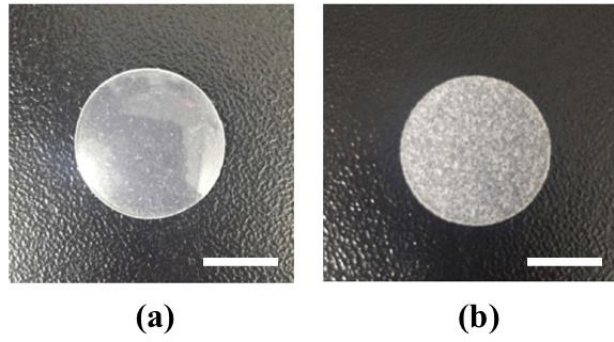


Figure 2.1 Optical images of the two types of silicone implants. Images of a sample from the (a) CF_S group and (b) CF_T group are shown.

2.2.3 *In vivo* experimental procedures

For *in vivo* animal experiments, 8-week-old SD rats weighing 250–300 g were used. The animals were housed under 12/12 h light/dark cycle conditions with free access to food and water. The *in vivo* protocols were approved by the Institutional Animal Care and Use Committee of Seoul National University Bundang Hospital (approval number: BA1603–196/011–01). To analyze the fibrosis pathway, animals were divided into two groups denoted by the surface type of the silicone implants: circular, flat, and smooth (CF_S); circular, flat, and textured (CF_T). I used at least five animals for each group, and at each predetermined time point, at least 20 animals were biopsied for analysis.

For implantation, animals were anesthetized via isoflurane (Hana Pharm, Seoul, Korea) inhalation. Then, the dorsal region was shaved and disinfected with betadine. To insert the implants, a 2–3 cm long incision was made with a surgical blade, and samples were inserted into the subcutaneous pocket. The incision site was then sutured with 4/0 nylon (Ethicon, NJ, USA). At the end of the implantation procedure, the surgical site was disinfected again with 70 % alcohol and betadine. All animals were fed for 8 weeks, and then, five animals from each group were randomly selected and sacrificed at predetermined time points (after 1, 2, 4 and 8 weeks) using carbon dioxide. For analysis, I obtained all the components of the surgical site (epidermis, dermis and capsule tissue, along with the implant).

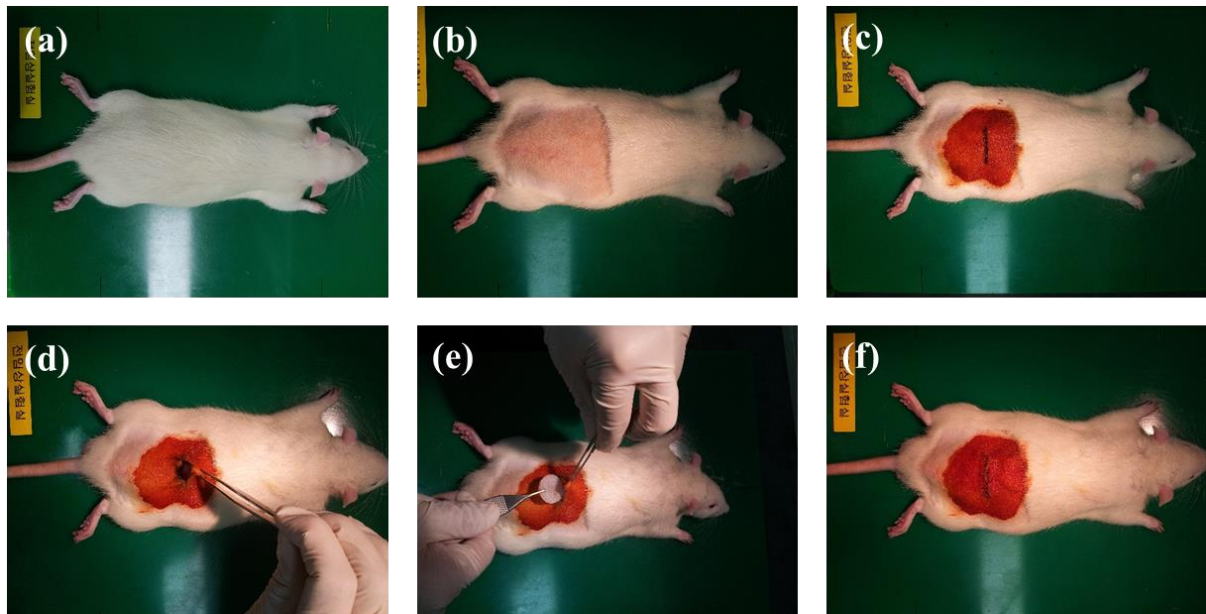


Figure 2.2 Surgical procedure for implant insertion in live rats.

Male Sprague–Dawley rats aged 9 weeks and weighing 250–300 g were used. The animals were fed sufficient water and food and housed with a 12/12 h light/dark cycle. All procedures were performed under an experimental protocol approved by the Institutional Animal Care and Use Committee at Seoul National University Bundang Hospital (BA1102–077/006–01). For implant insertion, (a) the animals were anesthetized using an intraperitoneal injection of a mixture of (0.1 ml/kg) Zoletil® 50 and Rompun® (1:1 v/v). (b) The surgical site was cleanly shaved . (c) Before the incision was made, the surgical site was marked with a surgical pen. (c) A 2–cm incision was made across the vertebral column, and (d) a pocket was made along the subpanniculus plane. (e) The implant sample was inserted in the pocket. (f) The incision was closed with 4–0 nylon (Ethicon, USA), and the surgical site was disinfected again with betadine.

2.2.4 Histological evaluation method

For the histological evaluation, all biopsied tissues were fixed in 4 % paraformaldehyde for 24 h. Then, the tissues were paraffinized and cut into 4- μm -slices for staining. First, the capsule thickness and inflammation were analyzed by staining the slide with H&E. For H&E staining, the sliced tissue was treated with a hematoxylin solution for 10 min and then washed with water for 5 min. Next, the slides were treated with 0.3 % v/v HCl and 70 % v/v ethanol and dipped into a 0.1 % v/v ammonium hydroxide solution. Finally, all slides were treated with an eosin Y solution and dehydrated with ethanol and xylene. To analyze the capsule thickness, I defined the thinnest region of the capsule from the peripheral region, and then, this region was observed at 50x magnification. [11,12] To score inflammation, H&E-stained images observed at 200 \times magnification was semi-quantitatively analyzed via a scoring method (0: none; 1: mild; 2: moderate; 3: severe). [13,14] All images were analyzed by a professional pathologist under a microscope (4x; Carl Zeiss, Germany). To analyze collagen density, slides were treated with a Biebrich scarlet-acid fuchsin solution. Then, the slides were washed with distilled water and a phosphotungstic-phosphomolybdic acid solution. Finally, the slides were stained with aniline blue solution and washed with tap water. After staining, I measured the positive blue signal in each image and calculated the blue signal area to determine collagen density. [38, 39] These area values were calibrated to the percentile value based on the total area of the images. All results were measured using the program ImageJ (National Institutes of Health, USA) [40].

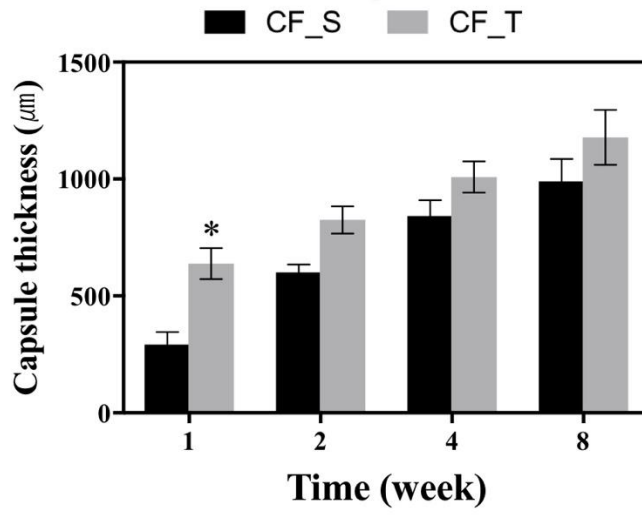
To analyze fibrosis-related cytokines and cells, including TGF- β , macrophages, myofibroblasts, and fibroblasts, immunofluorescence staining was performed using standard procedures with primary anti-TGF (1:250), anti-CD68 (1:150), anti- α smooth muscle actin (1:50), and anti-vimentin (1:200) antibodies, respectively. All stained images were obtained at 200 \times magnification (Imager A1; Carl Zeiss, Germany). For macrophages, myofibroblasts and fibroblasts, I counted the cells in the entire image. To assess the TGF- β score, I performed semi-quantitative

analyses using the following scores: 0: none; 1: mild; 2: moderate; and 3: severe. [38]

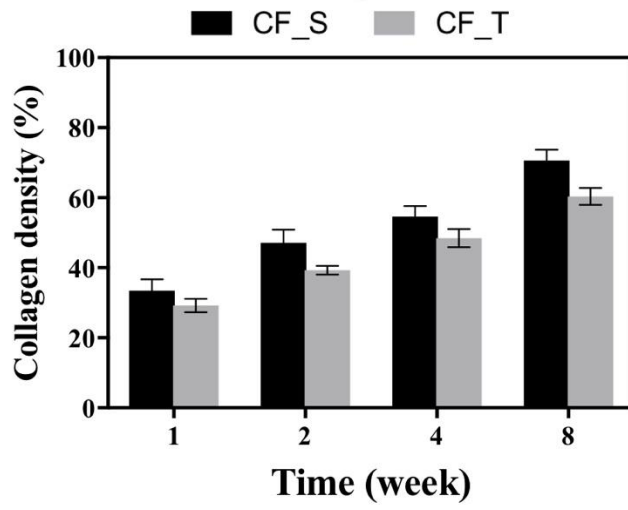
2.3 Overall information concerning fibrosis, cells and cellular factors

2.3.1 *In vivo* capsule thickness and collagen density

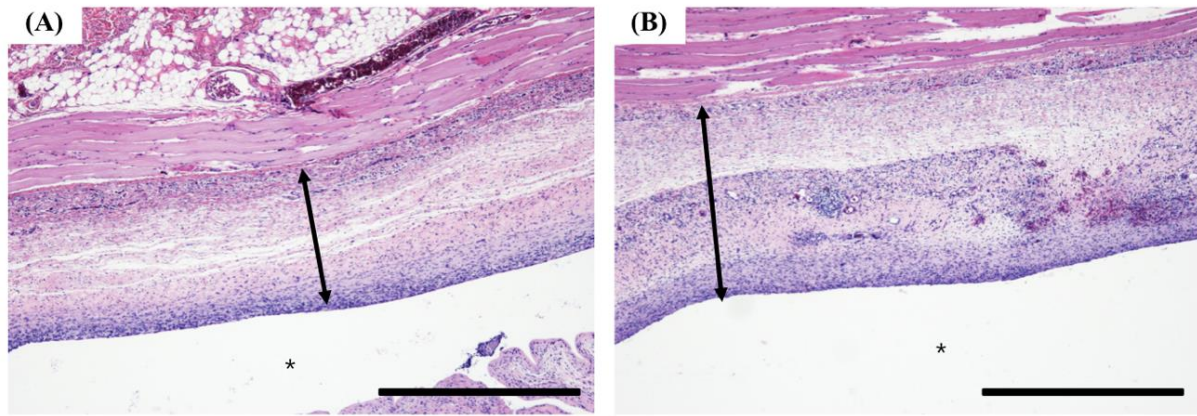
H & E tissue staining was performed to analyze capsule thickness, and at least five images per sample were obtained for analysis. Capsule thickness was significantly higher in the Texture group at 1 week, and the difference was observed for up to 8 weeks. However, the difference was not significant at 2 weeks, and only a higher tendency was observed than in the Smooth group. Collagen density analysis of tissue images was performed after MT staining. The collagen density tendency was the same as that of the capsule thickness profile, and it was confirmed that the collagen density continuously increased with time after implantation. Specifically, a lower collagen density was observed in the Texture group than in the Smooth group.



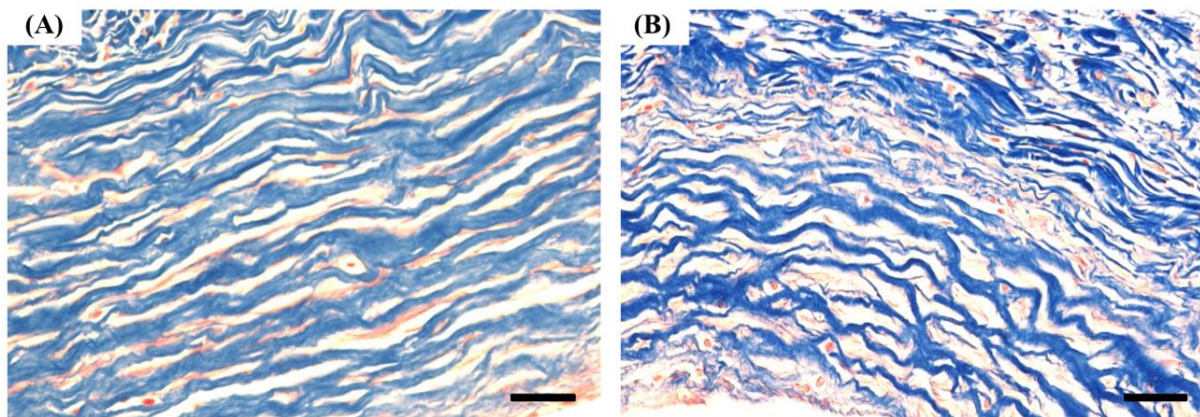
(a)



(b)



(c)

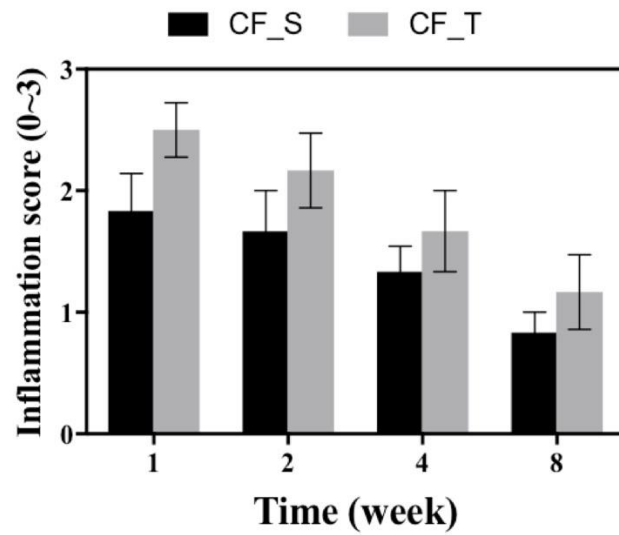


(d)

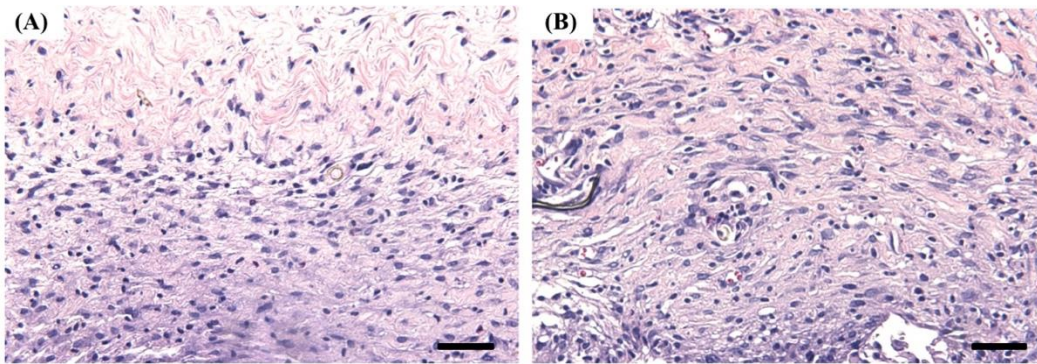
Figure 2.3 Evaluation of capsule thickness and collagen density around the implants. (a) Profiles of capsule thickness and (b) collagen density. (c–d) Representative stained images of capsule and collagen density at 8 weeks ((A), CF_S; (B), CF_T). The capsule thickness and collagen density image scale bars are 1 mm and 100 μm , respectively. The double-headed arrows indicate capsule thickness, and asterisks indicate the location of the implant insertion site.

2.3.2 Inflammation analysis

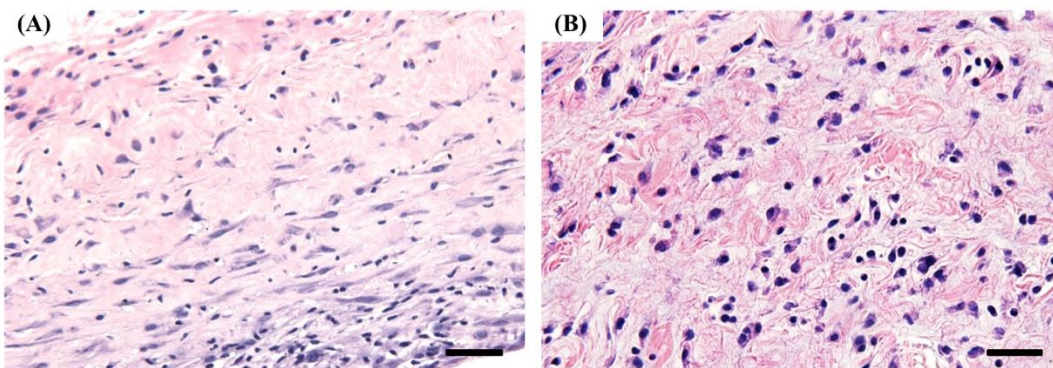
With regard to the inflammatory reaction, the CF_S and CF_T groups showed a strong inflammatory response at the first week, and a higher inflammatory response was observed in the CF_T group than in the CF_S group. However, the inflammatory score differences were not significantly different. At the initial stage after implantation, a high inflammatory reaction score is expected, which was predicted based on the immune response to the foreign material and the wound.



(a)



(b)

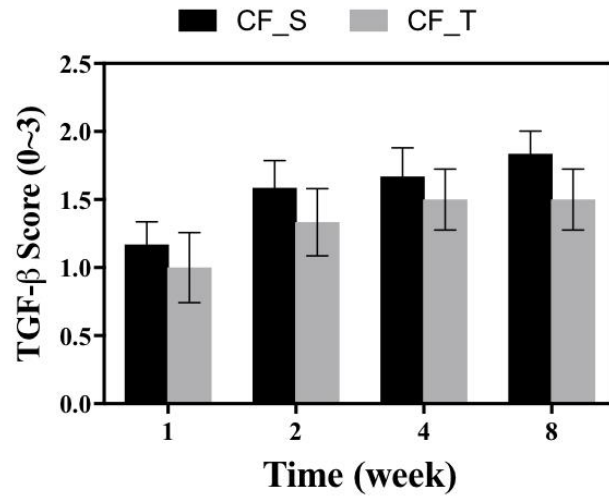


(c)

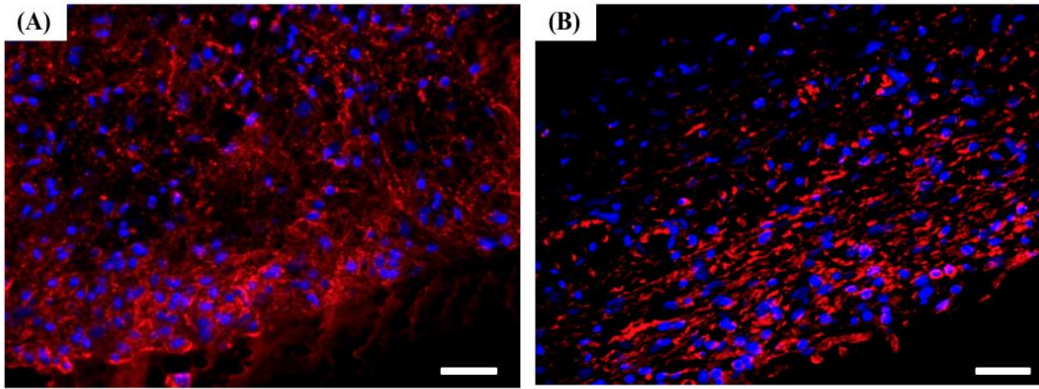
Figure 2.4 Evaluation of the inflammation score around the implants. (a) Profiles of the inflammation score and (b–c) representative stained images of the tissues biopsied at (b) 2 and (c) 8 weeks ((A), CF_S; (B), CF_T). The scale bars are 100 μ m.

2.3.3 Fibrosis-related factors

Fibrosis-related factors were analyzed, and TGF- β , fibroblast, and myofibroblast analyses were performed to examine changes in the fibrosis process. At week 1, TGF- β expression was observed to be low, but the expression increased until week 8. The TGF- β score was higher in the CF_S group than in the CF_T group, but the difference was not significant. ($p < 0.05$) (Fig. 2.4) Second, the number of fibroblasts and myofibroblasts, which are known to synthesize collagen, was determined, and the fibroblast cell numbers were lower in the CF_T group. I also observed that this tendency persisted for up to 8 weeks and confirmed that the increasing tendency was the same as that of the TGF- β score (Fig. 2.4). (Fig. 2.5) Myofibroblasts also showed the same tendency as TGF- β and the fibroblast number, showing a higher myofibroblast number in the CF_S group (Fig. 2.6).

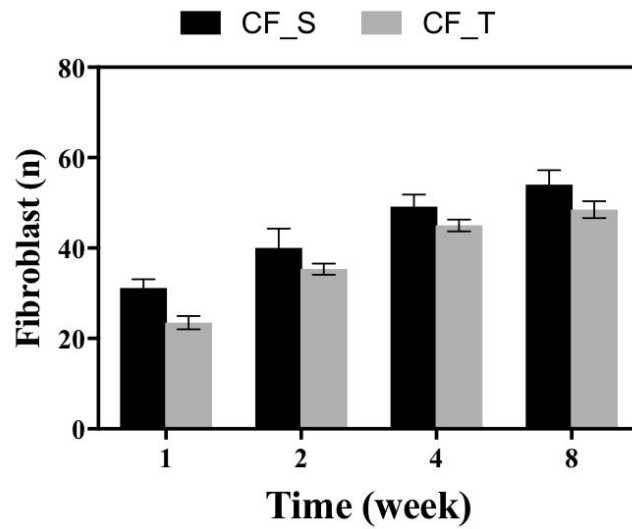


(a)

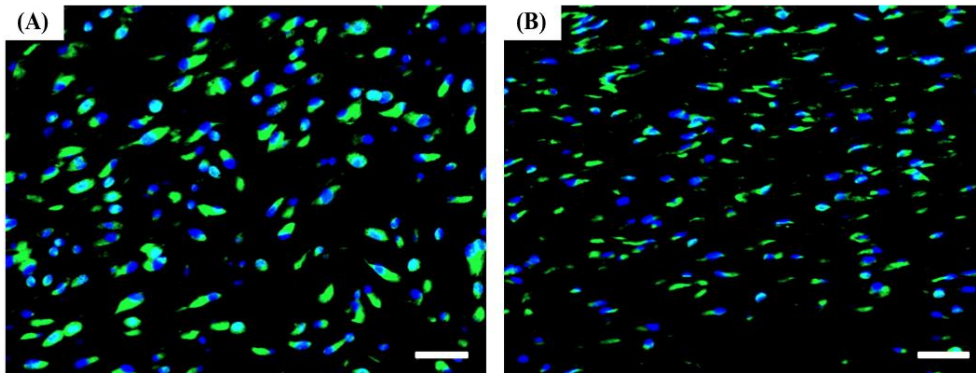


(b)

Figure 2.5 Evaluation of the TGF- β score. (a) Profiles of the TGF- β score and (b) representative stained images of the tissues biopsied at (b) 8 weeks ((A), CF_S; (B), CF_T). The scale bars represent 100 μ m.

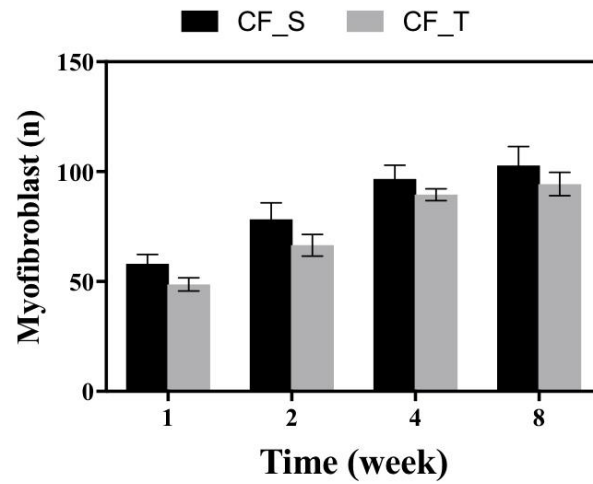


(a)

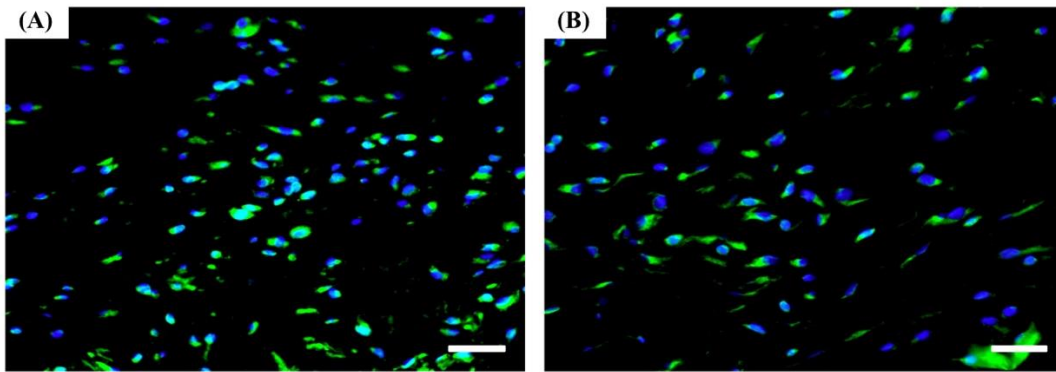


(b)

Figure 2.6 Evaluation of fibroblast cell numbers. (a) Profiles of the fibroblast cell number and (b) representative stained images of the tissues biopsied at 8 weeks ((A), CF_S; (B), CF_T). The scale bars represent 100 μm .



(a)



(b)

Figure 2.7 Evaluation of myofibroblast cell numbers. (a) Profiles of the myofibroblast cell numbers and (b) representative stained images of the tissues biopsied at 8 weeks ((A), CF_S; (B), CF_T). The scale bars represent 100 μm.

Chapter 3

Fibrosis suppression effect of montelukast in fibrosis pathway

3.1 Introduction

In the field of cosmetic and reconstructive surgery, silicone implants are one of the widely used medical devices [41, 42]. Although silicone implants are approved for clinical use, local complications, such as capsular contracture, implant rupture and gel bleeding, have not yet been fully resolved [24, 43]. One of the most serious complications is capsular contracture, which has been reported to occur in up to 30 % of patients after the insertion of silicone implants [25, 44]. When a silicone implant resides in the body for a prolonged period, excessive fibrous connective tissue, which is mainly composed of collagen and fibroblasts, accumulates around it, isolating the implant from the local tissue environment [33, 45]. Subsequently, a contractile force originating from the collagen and myofibroblasts, which are differentiated from fibroblasts, causes capsular contracture around the silicone implant. In serious cases, this can require a secondary surgery, which is highly inconvenient

for patients [10, 25].

This pathological phenomenon usually occurs because of a prolonged inflammation reaction, which leads to inflammation from acute to chronic stages [46]. In this case, the period of the acute inflammatory response can also be prolonged from days to weeks [47]. Once the silicone implant is inserted, acute inflammation initiates with infiltration of polymorphonuclear leukocytes (PMNs) from the blood vessels to the implant site [47]. Then, the PMNs secrete cysteinyl leukotrienes (CysLTs), which are potent inflammatory lipid mediators [48] and are also involved in the recruitment and survival of PMNs via autocrine and paracrine signaling [49, 50]. The persistent presence of the silicone implant leads to chronic inflammation, in which CysLTs stimulate the migration and proliferation of fibroblasts [32, 51]. During this chronic inflammation stage, fibroblasts differentiate into myofibroblasts and synthesize collagen, which is mediated by transforming growth factor (TGF)- β secreted by the fibroblasts themselves [52–54] and these lead to the capsule formation by fibrosis. Eventually, both the α smooth muscle actin (i.e., α -SMA) expressed on the myofibroblasts and the tension caused by the collagen fibrils are major causes of capsular contracture, i.e., a contractile force around the silicone implant [33, 55, 56].

Therefore, inhibiting CysLT production could be a strategy to prevent the formation of capsular contractures. Decreasing the number of CysLTs would reduce the recruitment and proliferation of fibroblasts, thereby decreasing the amount of myofibroblasts and collagen present during chronic inflammation. Montelukast is a potential therapeutic agent for the inhibition of CysLT production [16, 19]. Montelukast, a specific leukotriene receptor antagonist, selectively blocks the production of leukotriene D₄ (LTD₄) by binding to the type 1 CysLT receptor (CysLT1) located on the outer plasma membrane of the PMNs [16, 19, 57]. This drug has been reported to inhibit the accumulation of fibroblasts/myofibroblasts and the deposition of collagen [23, 58] and is already used clinically for the treatment of asthma or allergic diseases caused by CysLT overproduction [59–62].

Therefore, I suggest using the local, sustained release of montelukast around silicone implants to prevent capsular contracture. I hypothesize that the formation of the fibrous capsule, which occurs during chronic inflammation, can be reduced by inhibiting CysLT production even during the acute stage of inflammation, i.e., acute inflammation. Periodically early suppression of CysLT should decrease the amount of PMNs and thereby reduce the amount of CysLTs, which are secreted by the PMNs themselves. Decreasing the amount of CysLTs would result in less recruitment and proliferation of fibroblasts during chronic inflammation [51, 63], leading to reduced TGF- β secretion and less myofibroblast differentiation and collagen synthesis and, eventually, diminished capsular contracture. Therefore, I also hypothesize that this effect should increase as CysLT production is suppressed for longer periods, i.e., long-term montelukast exposure, during prolonged acute inflammation.

To examine our hypothesis, two distinct silicone implants were prepared in this work. For this, I differently coated the shell of silicone implants, already clinically available (SFS-LP, Hans Biomed, Korea), to give a silicone shell coated with montelukast only (i.e., the MON_SI) and one coated with a mixture of montelukast and poly (lactic-co-glycolic acid) (i.e., the PLGA_MON_SI). For the MON_SI, drug release was relatively short. For the PLGA_MON_SI, a longer drug release was achieved with the poly(lactic-co-glycolic acid) (PLGA) as a barrier against drug-diffusion [64, 65]. For controls without the drug, I also employed two different silicone implants: an uncoated, intact shell of a silicone implant (i.e., the SI) and a shell coated solely with PLGA (i.e., the PLGA_SI).

In this work, I assessed the *in vivo* effect of montelukast on anti-fibrosis as a function of the period of local drug release around the silicone implant. I inserted each of the different silicone implants in the subpanniculus plane of rats and biopsied the tissues around the implant at scheduled times for 12 weeks. The tissues were examined histopathologically with hematoxylin and eosin (H&E) staining, Masson's Trichrome (MT) staining and immunofluorescence (IF) staining. To examine the degree of the capsular contracture, I measured the tensile force at failure of the tissues (i.e., the

maximum force needed to break the tissue) around the implants at the end point (12 weeks) of the experiments.

3.2 Materials and methods

3.2.1 Materials

The shells of the clinically used silicone implants (SFS-LP) were a generous gift from Hans Biomed (Seoul, Korea). Montelukast was kindly donated by Daewoong Bio (Seoul, Korea). PLGA (inherent viscosity = 0.41 dl/g; LA:GA = 50:50) was obtained from Lakeshore Biomaterials (Birmingham, USA). I obtained dimethylformamide (DMF) from JT Baker (NJ, USA). EPO-TEK® 301-2 medical epoxy was purchased from Epoxy Technology (Billerica, USA). Tween 80 was obtained from Sigma-Aldrich (ME, USA). Zoletil 50 was purchased from Virbac (Fort Worth, TX, USA), and Rompun was obtained from Bayer (Leverkusen, Germany). Paraformaldehyde (4 %) was purchased from KCFC (Korea). For H&E staining, xylene, ethanol and hydrochloric acid (35 %-37 %) were purchased from Duksan Pure Chemicals (Ansan, Korea). Ammonia solution (28 %-30 %) was obtained from Junsie Chemical (Tokyo, Japan). Modified Mayer's H&E Y solutions were supplied by Richard-Allan Scientific (MI, USA). For MT staining, acetic acid (1 %) was obtained from Duksan Pure Chemicals (Ansan, Korea). Biebrich scarlet-acid fuchsin, phosphomolybdic acid, phosphotungstic acid and aniline blue solutions were purchased from Sigma-Aldrich (St. Louis, MO, USA). For IF staining, target-retrieval solution (10X) was purchased from Dako (Glostrup, Denmark). Anti-TGF- β (sc-146) was acquired from Santa Cruz Biotechnology (Dallas, TX, USA). Anti-vimentin (ab92547) and anti α -SMA (ab5694) were purchased from Abcam (Cambridge, MA, USA). Anti-CD163; ED2 (MCA342R) was obtained from AbD Serotec (Raleigh, NC, USA). Paraffin was supplied by Merck (USA).

3.2.2 Preparation of silicone implant samples

In this work, I fabricated four different types of implant samples using the shells of clinically used silicone implants (SFS-LP, Hans Biomed, Korea): intact implant shells (SI), implant shells coated with PLGA only (PLGA_SI), implant shells coated with montelukast (MON_SI) and implant shells coated with both PLGA and montelukast (PLGA_MON_SI). To prepare the SI, an implant shell, 1.5 mm in thickness, was first cut into a circle with a diameter of 2 cm. Then, the inner surfaces of two circular samples were bonded with medical epoxy (EPO-TEK[®] 301-2). Thus, the two outer surfaces of the shells were exposed to the surrounding tissues after insertion.

The other three samples were prepared by the following procedures. First, 10% w/v PLGA, 0.1% w/v montelukast or both 10% w/v PLGA and 0.17% w/v montelukast was dissolved in DMF to prepare the coating solutions for PLGA_SI, MON_SI and PLGA_MON_SI, respectively. Then, I sprayed the solution on the outer surface of a circular sample (2-cm diameter and 1.5-mm thickness) cut from the silicone implant shell. The spraying conditions are in the following: orifice diameter of the spraying nozzle: 0.8 mm; gap between the spraying nozzle and implant sample: 20 cm; pressure for spraying: 1.03 bar; and time for spraying: 2 s (also see Fig. S1 in the Supplementary Information). The sample was spray-coated twice with a drying interval of 30 min. Then, two of the coated samples were bonded, as described for the SI preparation. Finally, the coated samples were dried under vacuum for 24 h to fully remove the residual solvent.

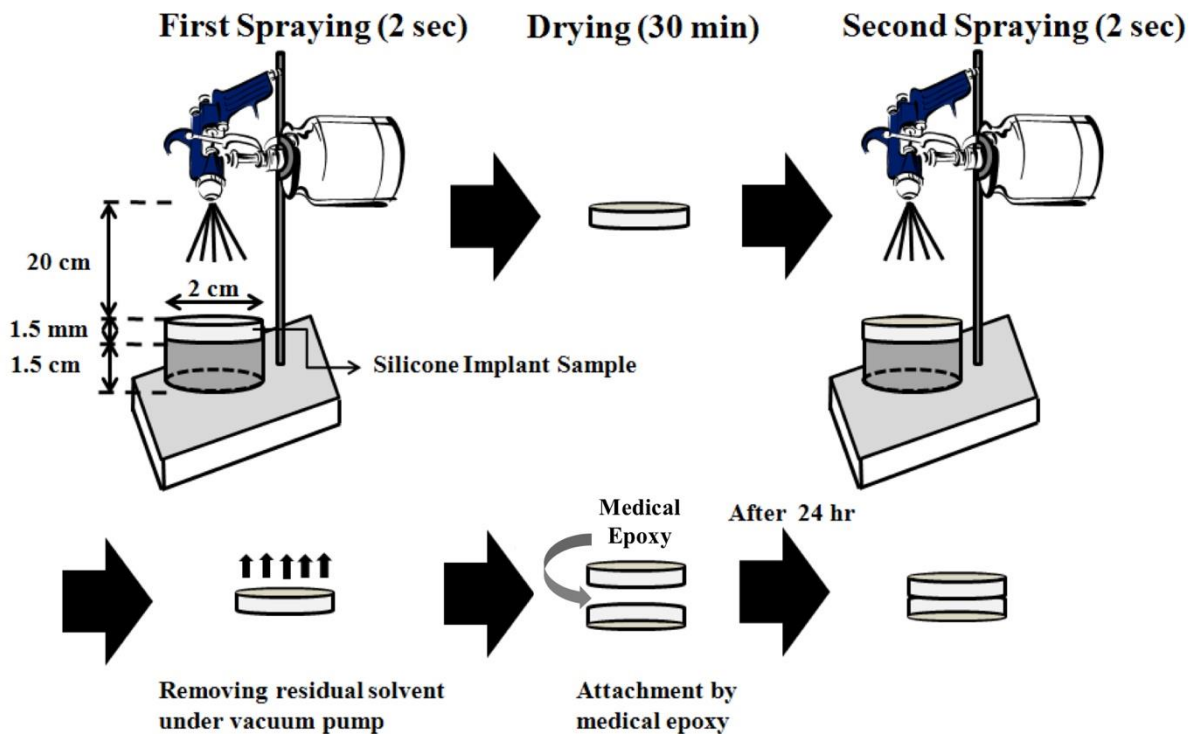


Figure 3.1 Schematic illustration of the preparation of the silicone implant samples.

3.2.3 Sample characterization

I imaged the implant samples with a scanning electron microscope (SEM; 7510F, Jeol, Japan). The chemical compositions of the implant samples were examined by Fourier transform infrared (FTIR) spectroscopy (JASCO 6100, Japan). For the FTIR analyses, each sample was milled with potassium bromide (KBr), which was then compressed into a thin pellet. Three distinct samples were measured for each implant type. To obtain the loading amount of montelukast in the MON_SI and PLGA_MON_SI, the sample was immersed in 10 ml DMF, which was sonicated for 60 min (NXPC-2010, KODO, Korea) to fully dissolve the drug. The aliquot was then assessed with a spectrophotometer (UV-1800, Shimadzu, Japan) at 335 nm. For each implant type, at least three samples were measured.

3.2.4 *In vitro* drug release study

The *in vitro* release profiles of montelukast of MON_SI and PLGA_MON_SI were examined. Each sample was immersed in 50 ml of phosphate-buffered saline (PBS; pH 7.4) containing 1 % v/v Tween® 80, which was continuously shaken at 125 rpm at 37 ° C (SI-300, JEO TECK, Korea). After a predetermined period, 10 ml of the release medium was collected, and an equal amount of the fresh medium was added back. The sampled media were each analyzed by spectrophotometry (UV-1800, Shimadzu, Japan) at 335 nm. For each implant type, the experiments were performed in triplicate.

3.2.5 *In vivo* experiment

For *in vivo* animal experiments, 9-week-old Sprague-Dawley rats weighing 250–300 g were

used. The animals were maintained in a 12/12 h light/dark cycle under specific–pathogen–free (SPF) conditions with free access to food and water. The approval for the experimental protocol was obtained by the Institutional Animal Care and Use Committee of Seoul National University Bundang Hospital (approval number: BA1102–077/006–01) and all procedures were performed in accordance with NIH Guide for the Care and Use of Laboratory Animals. In this study, the animals were divided into four groups according to the implant sample: animals inserted with the intact implants (SI group), animals inserted with the PLGA_SI (PLGA_SI group), animals inserted with the MON_SI (MON_SI group) and animals inserted with the PLGA_MON_SI (PLGA_MON_SI group). I assigned at least 25 animals to each of the animal groups.

For implant insertion, the animals were anesthetized by inhalation of isoflurane (Hana Pharm, Korea) and intraperitoneal injection of a 1 ml kg⁻¹ cocktail of Zoletil 50 and Rompun (1:1 v/v). Subsequently, the hair on the dorsal region was shaved, and the surgery site was disinfected with 70 % alcohol and betadine. Then, an incision (2–3 cm long) was made on the dorsal region with a #15 scalpel blade, and the implant was inserted into the subpanniculus pocket. The incision site was closed with a surgical suture (Nylon 4/0, Ethicon, USA). The surgical site was disinfected again with 70 % alcohol and betadine, and a light dressing was applied. After implantation, the animal was monitored for up to 12 weeks, as performed with the previous studies [66–68]. To assess the effect of montelukast–delivery period, I pursued to perform a more detailed analysis on the cascading events of inflammation. Thus, at predetermined times of 1, 2, 4, 8 and 12 weeks, five animals from each group were randomly selected for tissue biopsy. The animals were not marked and thus, at each biopsy time, a random number was generated to select a cage with two animals, among which one animal was randomly selected. For biopsy, the selected animals were sacrificed with carbon dioxide and the tissue in the dorsal region with the epidermis, dermis, posterior and anterior capsules, and the implant were removed.

3.2.6 Histological and IF evaluation

I fixed each of the biopsied tissues in paraformaldehyde (4%) for 24 h and then embedded it in paraffin. Then, I cut the paraffin block into 4- μm slices for staining. The detailed staining procedures are described in the Supplementary Information. After staining, a professional pathologist assessed each of the slides with a microscope (x4; Carl Zeiss, Germany). For each implant type and biopsy time, I obtained 5 stained-slides from each of the 5 animals, and thus, I statistically analyzed 25 stained-slides in this work.

The capsule thickness, number of inflammatory cells and collagen density were determined, as reported in our previous study [69]. To investigate the capsule thickness and number of inflammatory cells, the slides were subjected to H&E staining. I defined the capsule thickness as the thinnest region of the capsule from the sample image observed at 50x magnification [9, 70], where 25 stained-slides were statistically assessed for each implant type and biopsy time. To measure the number of inflammatory cells, the sample image at 400x magnification was obtained, and three distinct regions (0.12 mm² per region) were randomly selected within the capsule adjacent to the implant [71]. From each of the selected regions, the inflammatory cells (i.e., PMNs) were counted (Image J software (ver. 1.47), National Institutes of Health, USA), which were then summed and averaged. The collagen density around the implant was evaluated with MT staining. The area of the blue-stained collagen was measured using the sample image observed at 400x magnification with Image J software. The selected area was then calibrated to give the percentile value based on the whole area of the tissue in the same image [72].

To count the numbers of the cells, such as fibroblasts, macrophages and myofibroblasts, and assess the level of TGF- β expression, IF staining was performed with the primary anti-vimentin, anti-ED2, anti- α SMA and anti-TGF antibodies, respectively. Details of the IF staining procedure are presented in the Supplementary Information. From the stained slide, I obtained the fluorescent image at 200x

magnification (Imager A1; Carl Zeiss, Germany). For IF staining in this work, cell nuclei were stained with 4',6-diamidino-2-phenylindole (DAPI), fibroblasts and TGF- β were stained with Texas Red, and macrophages and myofibroblasts were stained with fluorescein isothiocyanate (FITC). Thus, two distinct fluorescent images (DAPI and Texas Red or DAPI and FITC) were obtained from each slide and were merged via Axiovision LE software (Carl Zeiss, Germany). From this merged image, I localized specific antigens in the capsule tissue around the implant [73]. For fibroblasts, macrophages and myofibroblasts, I counted the cells in the whole image. To assess TGF- β expression, I performed semiquantitative analyses by scoring as follows: 0: None, 1: Mild, 2: Moderate and 3: Severe.

3.2.7 Measurement of tissue tension

The tissue biopsied at 12 weeks after insertion was cut into a rectangular piece (1 cm x 3 cm, Fig. 3.2) that included the epidermis, dermis, posterior and anterior capsule adjacent to the implant. Then, the tensile force at failure was obtained by pulling both ends of the tissue sample at a rate of 3 mm/min using a universal testing machine (UTM; Instron-5543, MA, USA)[56].

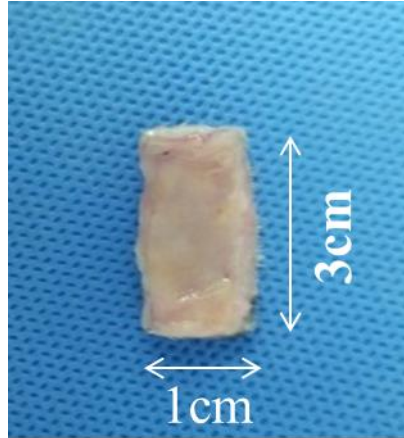


Figure 3.2 Representative image of the tissue biopsied from around the implant and used to measure tensile strength.

3.2.8 Statistical analysis

I first compared the experimental data among the four different groups with the Levene's test for equality of variances. Then, I performed a non-parametric Kruskal-Wallis test of the dependent variables, including the time at biopsy and the implant type. Thus, the capsule thicknesses, collagen densities, TGF- β levels, and numbers of PMNs, fibroblasts, myofibroblasts, macrophages and mast cells in the four groups (the SI, PLGA_SI, MON_SI and PLGA_MON_SI groups) were statistically analyzed via Kruskal-Wallis test and Bonferroni correction. Furthermore, I also compared the experimental data between the groups of MON_SI and PLGA_MON_SI at biopsy times of 1, 2, 4, 8 and 12 weeks using a Mann-Whitney U test to specifically assess the effect of the montelukast-release period. For all statistical analyses, P -values of < 0.05 were considered statistically significant.

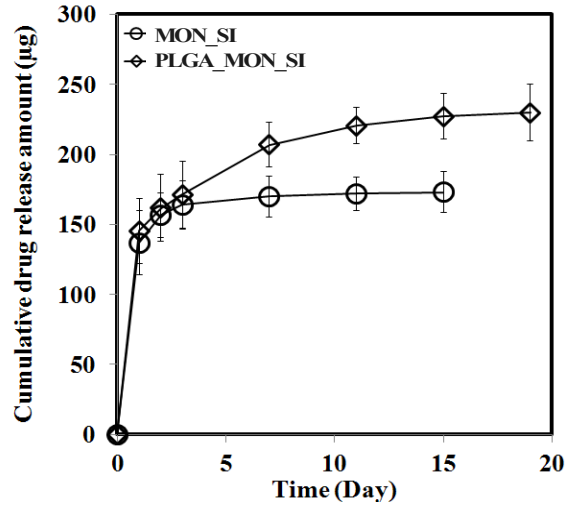
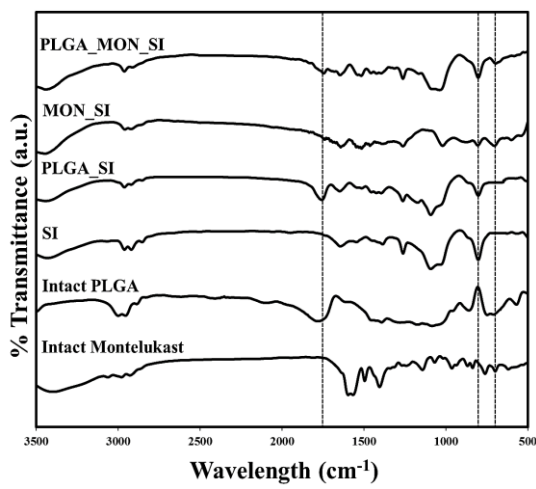
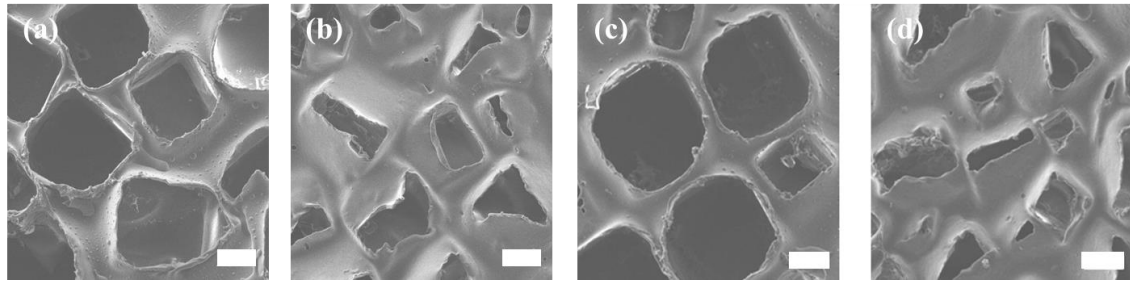
3.3 Results

3.3.1 Implant characterization

Fig 3.4(a–d) show the surface morphologies of the four different implants prepared in this work. The silicone implant that I used herein (SFS–LP, Hans Biomed, Korea) possesses a textured surface and thus, the SI shows a rough surface with rectangular wells of $206.82 \mu\text{m} \pm 19.68 \mu\text{m}$. The surface morphology of the MON_SI, i.e., the implant coated with the drug only, did not change substantially (Fig. 3.3(c)). In contrast, both PLGA_SI and PLGA_MON_SI showed a reduced size of the wells probably due to the presence of PLGA in the coating. (Figs. 3.3(b) and (d)). For the MON_SI and PLGA_MON_SI, the loading amounts of montelukast were $177.31 \pm 6.77 \mu\text{g}$ and $276.31 \pm 7.63 \mu\text{g}$, respectively (Table 1). Evaluating the FTIR spectra (Fig. 3.3(e)) revealed that intact montelukast exhibited a characteristic peak at approximately 700 cm^{-1} because of a meta–disubstituted aromatic ring [74]. For intact PLGA, a strong peak was found at 1750 cm^{-1} , which was attributed to the C=O stretching in the methane group [75]. The SI showed a strong peak at 800 cm^{-1} because of $\text{Si}(\text{CH}_3)_2$ groups derived from silicone [74]. For the coated MON_SI, PLGA_SI and PLGA_MON_SI samples, the characteristic peaks originated from each of the constituent materials were observed without any noticeable shifts, suggesting that the silicone, PLGA and montelukast co–existed as physical composites.

I also performed an *in vitro* drug–release study using the MON_SI and PLGA_MON_SI. As shown in Fig. 3.3(f), the drug was released in a sustained manner. The MON_SI released the drug over a short period (3 days) as the drug was loaded by simple absorption into the silicone matrix of the implant during spray–coating. After an apparent burst release of $22.81 \mu\text{g}/\text{cm}^2$ (77.32 %) on day 1, the drug was released with an approximate release rate of $2.18 \mu\text{g}/\text{cm}^2/\text{day}$ (7.38 %/day) for the rest 2 days. In contrast, because of the presence of PLGA in the coating, the PLGA_MON_SI released

the drug in a more sustained pattern for up to 15 days. For the first 3 days, the PLGA_MON_SI exhibited a similar pattern in drug-release amount as compared with the MON_SI: after an apparent burst release of $24.21 \mu\text{g}/\text{cm}^2$ (52.63 %) on day 1, the drug was released with an approximate release rate of $2.25 \mu\text{g}/\text{cm}^2/\text{day}$ (4.89%/day) for 2 days. For the remaining 12 days, the drug was released at a rate of $0.77 \mu\text{g}/\text{cm}^2/\text{day}$ (1.67 %/day).



(e)

(f)

Figure 3.3 Scanning electron micrographs of the surfaces of (a) SI, (b) PLGA_SI, (c) MON_SI and (d) PLGA_MON_SI. The scale bars are 100 μm . (e) FTIR spectra of the samples. The dashed lines indicate the characteristic peaks of interest. (f) *In vitro* drug release profiles of MON_SI and PLGA_MON_SI.

3.3.2 Capsule

To evaluate the effect of montelukast and its local-exposure period, I analyzed the capsule thicknesses among the four different animal groups, as shown in Fig. 3.4. At 1 week, the capsule thickness did not differ significantly among all tested groups because the capsule had not yet been fully formed by the fibrotic tissues; instead, it consisted of inflammatory cells, such as PMNs, in the very early stage of inflammation [76]. However, after 2 weeks, the effect of montelukast was noticeable. At 2–4 weeks, the capsule thicknesses were significantly thinner in the MON_SI and PLGA_MON_SI groups than in the SI group ($p < 0.05$). However, this effect did not persist for the MON_SI, possibly because of the relatively short period of drug exposure (Fig. 3.3(f)). Notably, the capsule thickness was consistently thinner in the PLGA_MON_SI group until 12 weeks. Indeed, at 2–12 weeks, the capsule thickness in this group was significantly thinner than that in the SI group. This difference was also significant relative to the MON_SI group. Throughout the testing period, the PLGA_SI group exhibited a capsule thickness profile similar to that of the SI group, as expected.

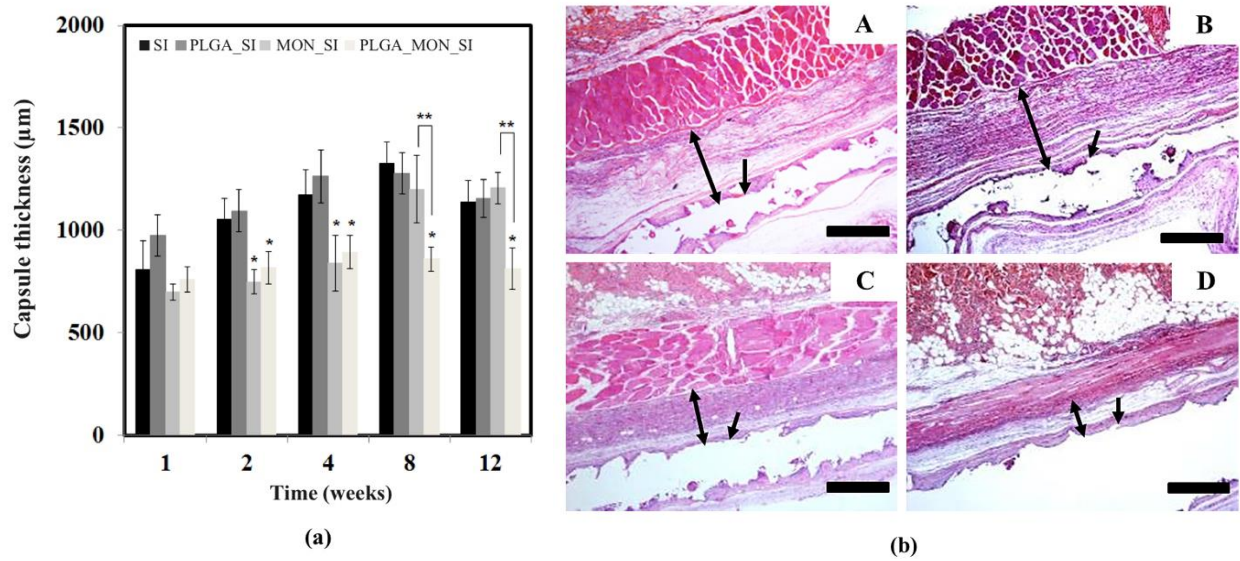


Figure 3.4 Evaluation of capsule thickness around the implants. (a) Profiles of capsule thickness and (b) representative stained images of the tissues biopsied at 12 weeks (A, SI; B, PLGA_SI; C, MON_SI; and D, PLGA_MON_SI). The scale bars are 1 mm. Asterisks (*) represent statistically significant differences compared with the SI group ($p < 0.05$). Double asterisks (**) represent statistically significant differences between the MON_SI group and PLGA_MON_SI group ($p < 0.05$). The double-headed arrows indicate the capsule thickness. The single-headed arrows indicate the location of the implants.

3.3.3 Collagen

I investigated the collagen density in the tissues biopsied from all testing groups by MT staining because the capsular contracture generally forms via pathological collagen deposition [13, 40]. As shown in Fig. 3.5, for the SI and PLGA_SI groups without montelukast, the collagen density continuously increased from 40–60 % to 90–96 %. This result could be attributable to the transition of inflammation from the acute to the chronic stage after the insertion of the silicone implant [7]. However, this pattern was not persistent in the presence of montelukast. For the MON_SI group, the collagen density did not increase until 4 weeks, and during this period, a significantly lower density was observed than that of the SI group. However, the collagen density increased dramatically at 8–12 weeks and became not substantially different from that of the SI group. Again, this could be attributed to the short-term montelukast exposure (Fig. 3.3(f)). A notable difference was observed for the PLGA_MON_SI group, which showed no apparent increase in collagen density during the testing period. Beginning after 2 weeks, the collagen density in this group was significantly lower than that of the SI group. Compared to that in the MON_SI group, the collagen density was significantly lower at 8 and 12 weeks.

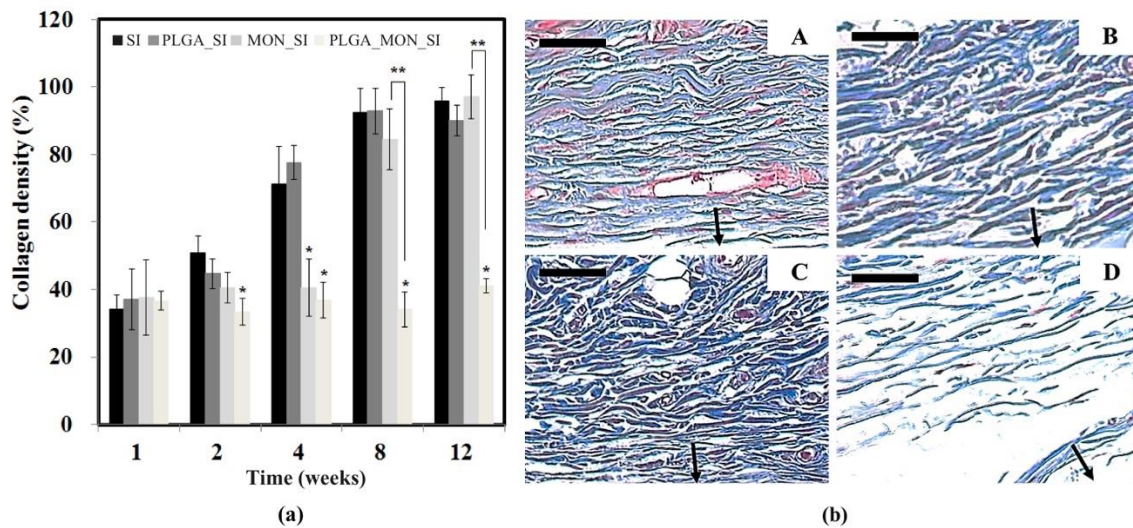


Figure 3.5 Evaluation of collagen density around the implants. (a) Profiles of collagen density and (b) representative stained images of the tissues biopsied at 12 weeks (A; SI, B; PLGA_SI, C; MON_SI and D; PLGA_MON_SI). The scale bars are 100 μm. Asterisks (*) represent statistically significant differences compared with SI group ($p < 0.05$). Double asterisks (**) represent statistically significant differences between the MON_SI and PLGA_MON_SI groups ($p < 0.05$). The black arrows indicate the location of the implants.

3.3.4 Inflammatory cells

Montelukast is known to decrease CysLTs [16, 19], which should directly affect the recruitment and survival of the PMNs by suppressing autocrine and paracrine signaling [49, 50]. To examine this effect, I evaluated the number of inflammatory cells, i.e., PMNs, using H&E staining [48]. As shown in Fig. 3.6, the number of PMNs continuously decreased in all samples, indicating the gradual disappearance of acute inflammation. A relatively higher number of PMNs was observed even until 2 weeks, indicating that the silicone implants caused prolonged acute inflammation. The presence of montelukast evidently decreased the number of PMNs. In the MON_SI group, the PMN number was significantly lower at 1–2 weeks but did not differ from that of the SI group. However, the PLGA_MON_SI group, which was subjected to long-term montelukast exposure, exhibited a lower number of PMNs throughout the testing period, and the PMN number in this group was significantly lower than that in the SI group. Additionally, compared with the MON_SI group, the PMN number was significantly lower at 4–12 weeks.

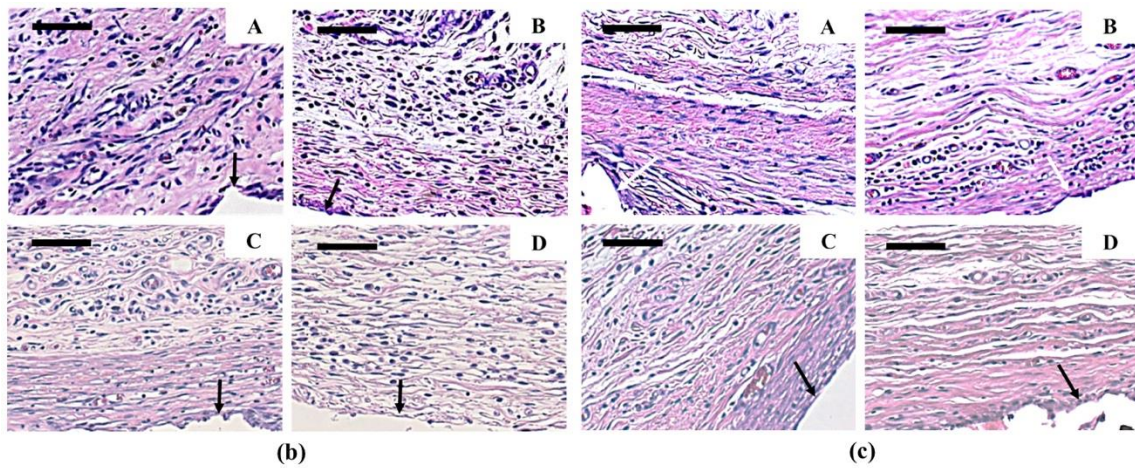
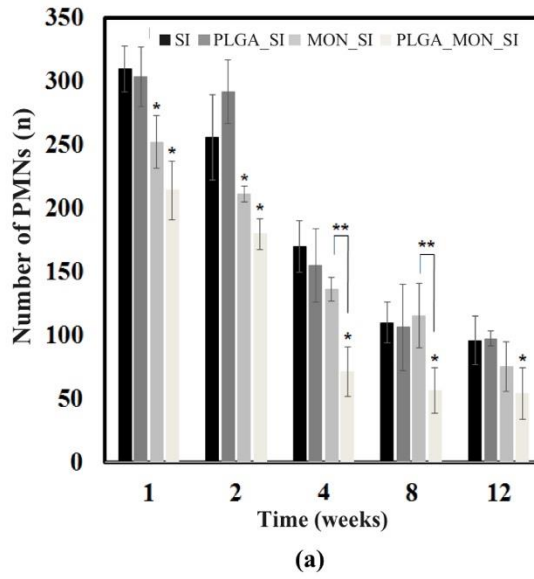


Figure 3.6 Evaluation of the number of inflammatory cells (PMNs) around the implants. (a) Profiles of PMN number and (b, c) representative stained images at 2 and 4 weeks, respectively (A; SI, B; PLGA_SI, C; MON_SI and D; PLGA_MON_SI). The scale bars are 100 μm . Asterisks (*) represent statistically significant differences compared with the SI group ($p < 0.05$). Double asterisks (**) represent statistically significant differences between the MON_SI group and PLGA_MON_SI group ($p < 0.05$). The arrows indicate the locations of the implants.

3.3.5 Fibroblast

CysLT influences the migration and proliferation of fibroblasts [32, 51], which are known to play a major role in collagen synthesis and which differentiate into myofibroblasts, causing tension and inducing capsule contracture [77]. Therefore, I examined the effect of montelukast on fibroblasts around the silicone implant, as shown in Fig. 3.7. For the SI and PLGA_SI groups, the number of fibroblasts gradually increased until 12 weeks. In contrast, in the MON_SI group, the fibroblast number did not increase substantially until 4 weeks and was significantly lower than that in the SI group. However, a dramatic increase in the number of fibroblasts occurred after 8 weeks, and the number became comparable to that in the SI group. In the PLGA_MON_SI group, I observed the lowest number of fibroblasts and beginning after 2 weeks, this was consistently significantly lower compared with that of the SI group. The fibroblast number in this group was also significantly lower than those of the MON_SI group at 8 and 12 weeks.

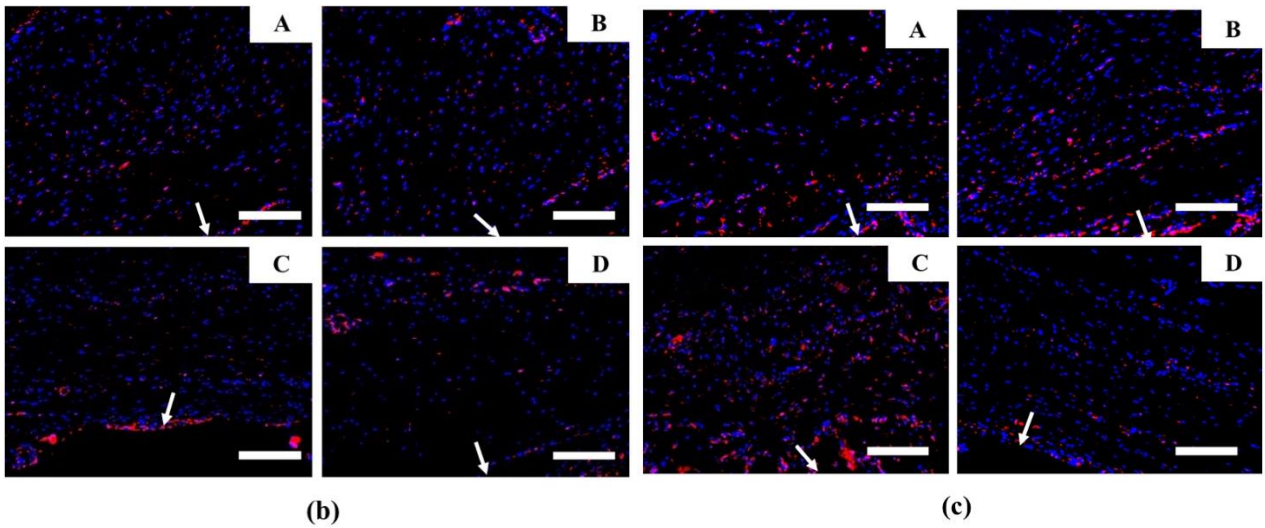
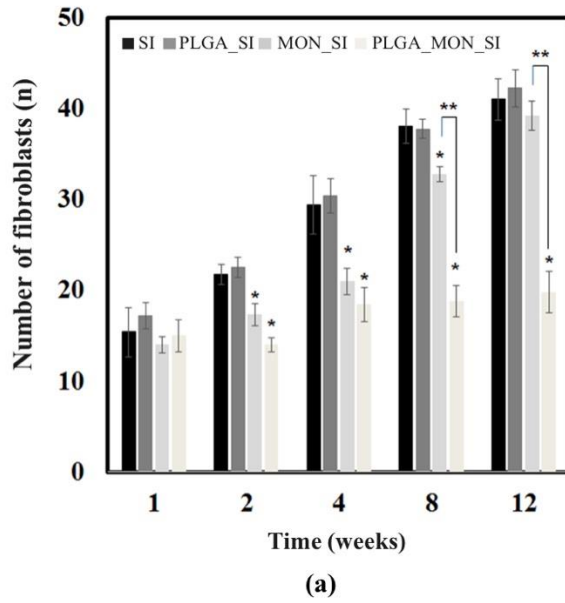
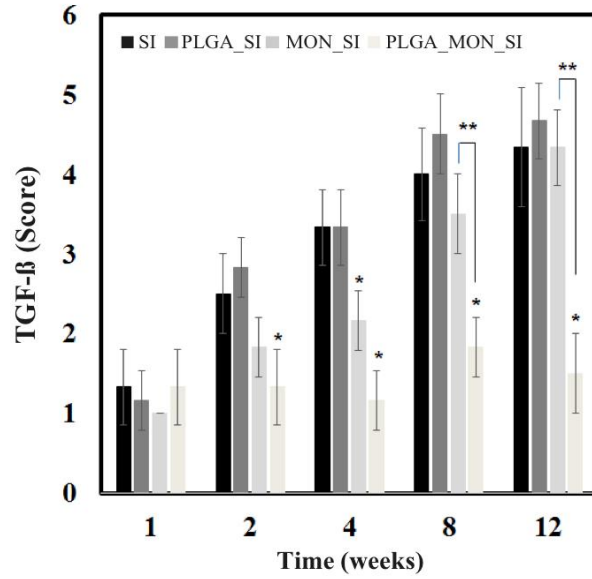


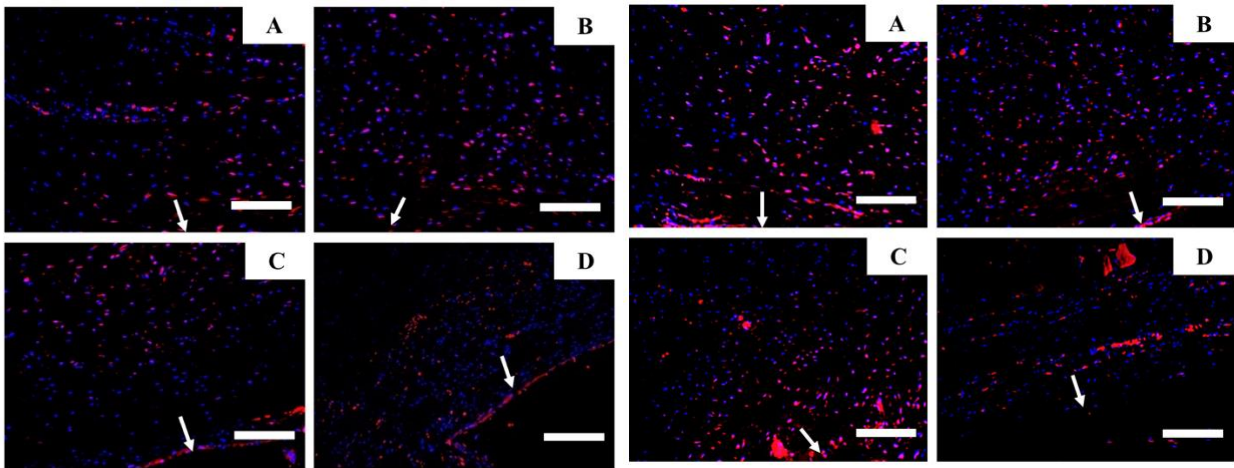
Figure 3.7 Evaluation of the number of fibroblasts around the implants. (a) Profiles of fibroblast numbers and (b, c) representative stained images at 4 and 12 weeks, respectively (A; SI, B; PLGA_SI, C; MON_SI and D; PLGA_MON_SI). The cells stained with both DAPI and Texas red were selectively counted for analysis. The scale bars are 200 μm . Asterisks (*) represent statistically significant differences compared with the SI group ($p < 0.05$). Double asterisks (**) represent statistically significant differences between the MON_SI group and PLGA_MON_SI group ($p < 0.05$). The arrows indicate the locations of the implants.

3.3.6 TGF- β

I assessed the level of TGF- β expression because it is a major cytokine secreted by fibroblasts [78]. According to our semi-quantitative analysis shown in Fig. 3.8, the TGF- β expression level continuously increased in the groups without montelukast, i.e., the groups of SI and PLGA_SI. The highest expression, which was found at 12 weeks, suggests active fibrosis and appeared to be correlated with thick-capsule formation with dense collagen (Figs. 3.4 and 3.5). In the MON_SI group, the TGF- β expression level did not increase as much, and it was significantly lower than that in the SI group at 4 weeks. However, beginning after 8 weeks, the TGF- β expression level dramatically increased and became similar to that of the SI group, possibly because of the short-term montelukast exposure. Meanwhile, the PLGA_MON_SI group showed no apparent increase in TGF- β expression level, which was continuously significantly lower than that of the SI group beginning after 2 weeks. This difference was also apparent relative to the MON_SI group at 8 and 12 weeks.



(a)



(b)

(c)

Figure 3.8 Evaluation of the level of TGF- β expression around the implants. (a) Profiles of the level of TGF- β expression and (b, c) representative stained images at 4 and 12 weeks, respectively (A; SI, B; PLGA_SI, C; MON_SI and D; PLGA_MON_SI). Cells stained with both DAPI and Texas red were selectively assessed for grading. The scale bars are 200 μ m. Asterisks (*) represent statistically significant differences compared with the SI group ($p < 0.05$). Double asterisks (**) represent statistically significant differences between the MON_SI group and PLGA_MON_SI group ($p < 0.05$). The arrows indicate the locations of the implants.

3.3.7 Macrophages

Macrophages also secrete TGF- β during the late-stage inflammation [51]. Therefore, I assessed the number of macrophages and examined its correlation with the observed TGF- β expression level (Fig. 3.8). As shown in Fig. 3.9, the number of macrophages did not vary significantly among the tested samples and biopsy times, [25], implying that the profile of TGF- β expression was not highly correlated with the number of macrophages.

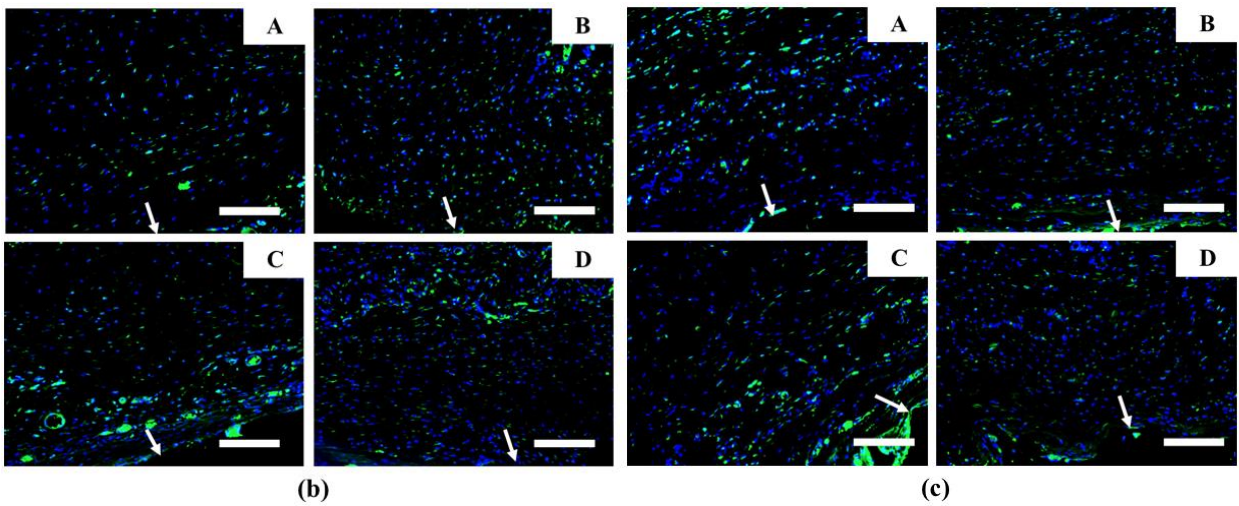
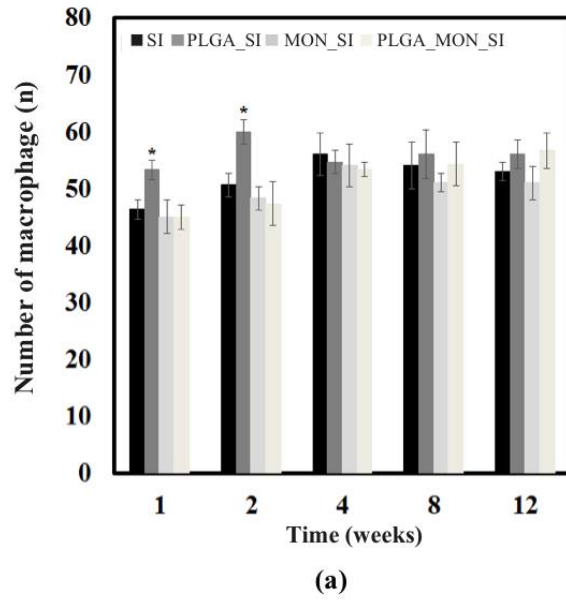


Figure 3.9 Evaluation of the number of macrophages around the implants. (a) Profiles of macrophage numbers and (b, c) representative stained images at 4 and 12 weeks, respectively (A; SI, B; PLGA_SI, C; MON_SI and D; PLGA_MON_SI). Cells stained with both DAPI and FITC were selectively counted for analysis. The scale bars are 200 μm . Asterisks (*) represent statistically significant differences compared with the SI group ($p < 0.05$). Double asterisks (**) represent statistically significant differences between the MON_SI and PLGA_MON_SI groups ($p < 0.05$). The arrows indicate the locations of the implants.

3.3.8 Myofibroblasts

I assessed the number of myofibroblasts in the capsule tissue around the silicone implant because these cells are known to induce contraction during fibrosis [42]. As shown in Fig. 3.10, in the absence of montelukast, the number of myofibroblasts gradually increased in the SI and PLGA_SI groups until 12 weeks. The number of myofibroblasts in the MON_SI group was significantly lower than that in the SI group at 2 and 4 weeks; however, subsequently, the number of myofibroblasts rebounded and became similar to that of the SI. Notably, because of long-term montelukast exposure in the PLGA_MON_SI group, the number of myofibroblasts did not increase substantially and was significantly lower than that in the SI group after 2 weeks. It was significantly lower than that of the SI group at 8 and 12 weeks.

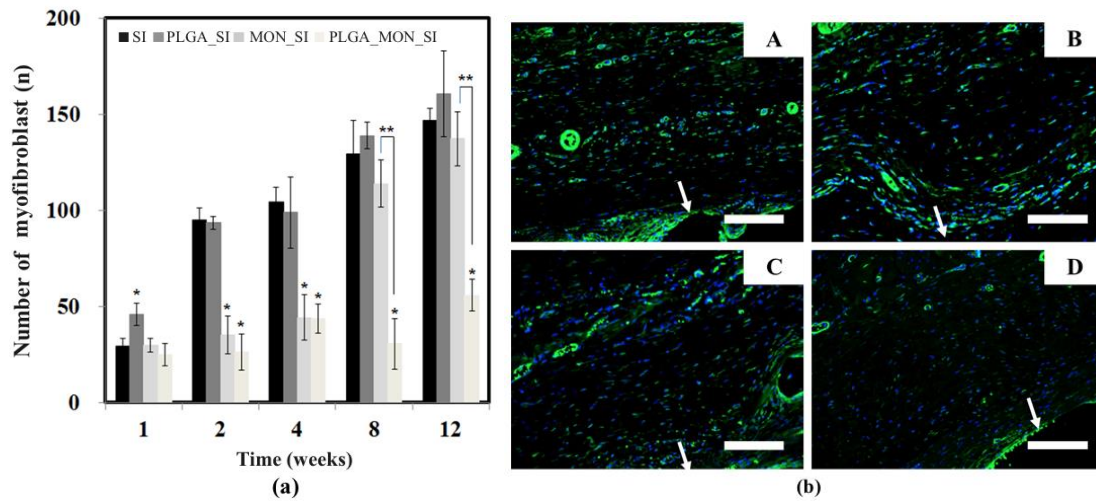


Figure 3.10 Evaluation of the number of myofibroblasts around the implants. (a) Profiles of myofibroblast numbers and (b) representative stained images at 12 weeks (A; SI, B; PLGA_SI, C; MON_Si and D; PLGA_MON_SI). Cells stained with both DAPI and FITC were selectively counted for analysis. The scale bars are 200 μm . Asterisks (*) represent statistically significant differences compared with the SI group ($p < 0.05$). Double asterisks (**) represent statistically significant differences between the MON_SI and PLGA_MON_SI groups ($p < 0.05$). The arrows indicate the locations of the implants.

3.3.9 Tissue tension

Contraction of the capsule tissue is the pathological indication of fibrosis around a silicone implant [2]. To assess this contraction, I measured the tensile force at break in the tissues biopsied at the experimental end point (12 weeks). As shown in Fig. 3.11 (Table 3.1), the tensile force at break in the PLGA_MON_SI was significantly lower, compared with that in the SI group. For the PLGA_SI and MON_SI groups, the tensile force did not differ significantly and was similar to that of the SI group.

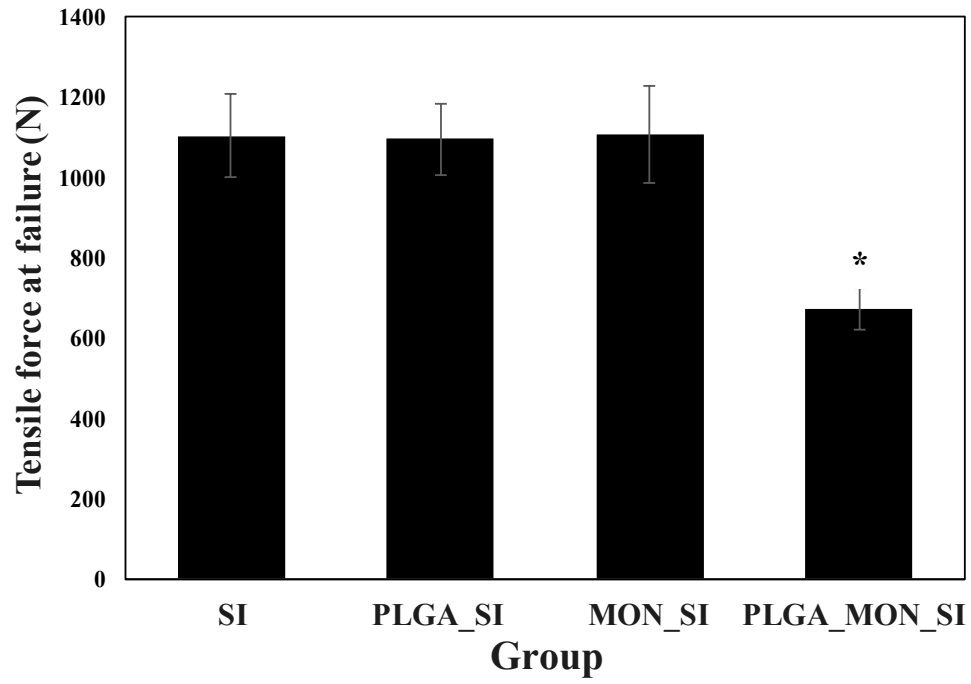


Figure 3.11 Tensile force at failure of the tissue adjacent to the implant biopsied at 12 weeks after implantation. The asterisk (*) represents a statistically significant difference compared with the SI group ($p < 0.05$).

Table 3.1 Tensile force at failure of tissue

Sample Types	Tensile force at failure (N)
SI	1104 ± 102
PLGA_SI	1095 ± 90
MON_SI	1107 ± 120
PLGA_MON_SI	672 ± 54

Values are the mean ± SD.

3.4 Discussion

Capsular contracture has been regarded as one of the most troublesome complications with a silicone implant [10]. Capsule contracture is generally mediated by a foreign body reaction that occurs from the acute to chronic inflammation stages and eventually isolates and encapsulates the silicone implant with fibrous tissues [7]. During this inflammation process, in this work, I focused on the role of a type of potent inflammatory lipid mediator, CysLTs. CysLTs are mainly secreted from PMNs and stimulate the recruitment and proliferation of fibroblasts [48, 51, 63]. Fibroblasts secrete TGF- β , which activates fibroblasts to promote collagen synthesis and stimulates the differentiation of fibroblasts into myofibroblasts [32, 33, 79]. In addition to the excessive accumulation of collagen, myofibroblasts create a contractile force in the capsule tissue around the silicone implant [80], resulting in fibrotic capsular contracture.

Our results showed that montelukast reduced the number of PMNs (Fig. 3.6). This finding implied that CysLT production decreased as the PMNs secrete CysLTs and the PMNs are also recruited via autocrine and paracrine signaling based on CysLTs [49, 50]. I also showed that as the length of montelukast exposure increased, this effect became more prominent throughout the 12-week testing period. Interestingly, a significant decrease in the PMN number was observed after the period of montelukast release from the implants ended (Fig. 3.3(f)). The MON_SI and PLGA_MON_SI released montelukast for 3 and 15 days, respectively and for the first 3 days, both implants released a similar amount of montelukast. However, the PMN number exhibited significant decreases for much longer: 2 and 12 weeks, respectively. The decrease in PMNs should reduce the level of CysLT secretion, thereby further reducing PMN recruitment. This effect could be more prominent as the degranulation of mast cells would also decrease with exposure of montelukast [81–83] although the number of mast cells did not appear to be influenced significantly. This cascade appeared to be accumulated to prolong the reduction of both PMNs and CysLT even after

montelukast release ended. Therefore, its effect increased as the length of montelukast exposure increased.

In this study, as CysLT production was suppressed, the number of fibroblasts also decreased [32, 51], and longer periods of CysLT suppression amplified this effect (Fig. 3.7). In the PLGA_MON_SI group, the significantly lower number of fibroblasts was observed throughout the 12-week testing period. However, for the shorter release period, the number of fibroblasts increased, and it significantly differed from that of the SI group at 12 weeks. Our results also showed that TGF- β expression and the number of myofibroblasts were highly correlated with the number of fibroblasts (Figs. 3.7, 3.8 and 3.10). It was reported that more CysLT receptors are present with fibroblasts than with macrophages [84]. Probably because of this, with the dose of montelukast that I employed in this study, the number of macrophages did not vary significantly (Fig. 3.9). Therefore, ruling out TGF- β secretion from macrophages, a decrease in TGF- β expression is mainly attributable to the reduced number of fibroblasts [78], which also decreased the numbers of differentiated cells, i.e., myofibroblasts [32, 85].

Therefore, I propose the sustained, local suppression of CysLT with montelukast as a strategy to reduce capsule formation around silicone implants. Although a longer-term study would provide with more information, our 12-week study still suggested that the periodically early suppression of CysLT production could reduce capsule thickness (Fig. 3.4) and collagen density (Fig. 3.5) during the later stage of inflammation. Some previous studies also reported that the fibrotic capsule formation around the silicone implant could be still reduced when a leukotriene receptor antagonist was injected once at the time of implantation [67, 68]. More importantly, I suggest that the effectiveness of this method could be increased by prolonging the montelukast exposure (Fig. 3.3(f)). Thus, sustained CysLT suppression could continuously reduce the number of fibroblasts (Fig. 3.7), thereby decreasing TGF- β expression (Fig. 3.8), collagen synthesis and differentiation into myofibroblasts (Figs. 3.5 and 3.10). These effects would then contribute to decreasing the tension in the capsule tissue during the

later stage of inflammation (Fig. 3.11).

In our previous study [69], I employed a TGF- β inhibitor, tranilast, for local, sustained delivery around the silicone implant, where a thinner capsule composed of less dense collagen was obtained, as compared with the results in this current study. By suppressing TGF- β directly, the numbers of both macrophages and fibroblasts reduced and they are known to be responsible for production of TGF- β at the later stage of inflammation [14]. Therefore, reduction of TGF- β became more pronounced, hence further reducing the number of fibroblasts and collagen synthesis. On the other hand, our current study revealed that the number of macrophages did not vary significantly among tested samples (Fig. 3.9) and only fibroblasts were seen to reduce with montelukast-delivery (Fig. 3.7). Therefore, to be more effective, I envision the use of a higher dose or a longer-term release of montelukast around the silicone implant.

In clinical settings, a leukotriene receptor antagonist drug, such as montelukast and zafirlukast, has been prescribed for oral administration to mitigate capsular contracture [66, 86]. However, to be effective, a long-term montelukast regimen (~6 months) is often required accompanied by systemic drug exposure [87], which may cause unexpected adverse side effects, such as headache, pain or dizziness [88]. Thus, one potential advantage of our strategy is that it involves local montelukast exposure for a relatively short period covering the early stage of inflammation. Our results revealed that capsular contracture can be reduced, even using relatively low doses of montelukast. Indeed, the PLGA_MON_SI provided a mean daily dose of 2.41 $\mu\text{g}/\text{cm}^2$, which corresponds to approximately 1.20 mg/day for a human-use silicone implant with an overall surface of $\sim 500 \text{ cm}^2$ [89]. In comparison, the recommended oral dose of montelukast is approximately 10 mg/day.[87, 90].

3.5 Conclusion

I propose that the long-term, local suppression of CysLTs during the period of early-stage inflammation as a strategy to mitigate the capsular contracture around silicone implants. Our findings showed that the PLGA_MON_SI, which released montelukast, a CysLT receptor antagonist, for 15 days, significantly reduced the capsule thickness, collagen density and mechanical stiffness of the tissue biopsied at 12 weeks after implant insertion in living rats compared to an intact implant without montelukast. Local montelukast exposure reduced the number of PMNs, implying decreased CysLT secretion. Because of the mutual reduction effect of PMNs and CysLT, this phenomenon appeared to extend even after the release of montelukast was complete, which was more prominent with longer montelukast exposures. Therefore, fibroblast recruitment was continuously hindered, leading to a decreased TGF- β quantity and the presence of fewer myofibroblasts in the capsule tissue during the period of later-stage inflammation and, eventually, reduced capsular contracture. Therefore, I conclude that the sustained release of montelukast at the local insertion site represents a promising way to reduce capsular contracture around silicone implants.

Chapter 4

Analysis of macrophage phenotype changes induced by montelukast in the fibrosis pathway

4.1 Introduction

Fibrosis progression is a multistep process, and macrophages associated with the fibrosis pathway are known to be activated throughout the entire inflammatory period (acute and chronic inflammation). Macrophages express various activating factors (e.g., interleukin family members, TNF- α , IFN- γ , and TGF- β) and change into FBGCs, which cause fibrosis. FBGCs, as well as various other macrophages, are reported to be involved in all stages of inflammation and the immune response [8, 33].

Currently, macrophages are divided into two broad phenotypes: "classically activated" macrophage (M1 phenotype) and "alternatively activated" macrophages (M2 phenotype). These two types of macrophages exhibit different activities. Classically activated M1 macrophages have been shown to be inducible in many cases due to the influence of the early inflammation factors IFN- γ

and TNF- α and have microbicidal activity. In addition, the effects of these cytokines increase inflammatory cell activity, and M1 macrophages release high levels of pro-inflammatory cytokines. Specifically, classically activated (M1) macrophages produce IL-1, IL-6, and IL-23, which affect the proliferation and differentiation of TH₁₇ cells [91-93]. TH₁₇ cells express IL-17, thereby increasing the number of PMNs and amplifying the inflammatory response [94]. M1 macrophage activation is expected to increase the inflammatory response during fibrosis, thereby accelerating fibrosis.

Alternatively activated [M2] macrophages express IL-4 and IL-13 and regulate the production of inflammatory cytokines, and the polyamines expressed by M2 macrophages suppress pro-inflammatory cytokine production [95]. In addition, M2 macrophages suppress the differentiation of immune lymphocytes, have an indirect inhibitory effect on the immune response (foreign body reaction) and regulate the inflammatory response through abundant expression of IL-10 [96, 97]. In summary, classically activated (M1) macrophages induce inflammatory responses in tissues and can lead to excessive inflammation in host tissues. Conversely, alternatively activated (M2) macrophages regulate abnormal inflammatory responses through a variety of immune suppression mechanisms via IL-4, IL-13 and IL-10 expression [95].

In this chapter, I examined the effect of montelukast on macrophage phenotype diversity and evaluated the M1/M2 macrophage ratio in response to controlled drug delivery, which showed that montelukast inhibited fibrosis.

4.2 Materials and methods

4.2.1 Materials

For IF staining, target-retrieval solution (10X) and antibody diluent were purchased from Dako (Glostrup, Denmark). Anti-CD68 (ab955), anti-CD80 (ab215166) and anti-CD163 (ab182422) antibodies were obtained from Abcam (Cambridge, MA, USA).

4.2.2 Histological evaluation

I performed IF staining to assess the number of M1 and M2 macrophages. The primary antibodies and the diluting conditions employed in this work were as follows. For total macrophages, the anti-CD68 mouse antibody was diluted 1:150. For both the M1 and M2 macrophage analyses, the anti-CD80 rabbit antibody and anti-CD163 antibody were diluted 1:250 respectively. For secondary antibodies, anti-rabbit and anti-mouse antibodies were used and diluted 1:2000. All dilutions were performed with an antibody diluent.

To determine the number of macrophages, IF staining was performed with primary antibodies. From the stained slides, I obtained fluorescence images at 200x magnification (Imager A1; Carl Zeiss, Germany). Cell nuclei were stained with 4',6-diamidino-2-phenylindole (DAPI), total macrophages were stained with Texas Red, and M1 and M2 macrophages were stained with fluorescein isothiocyanate (FITC). Thus, two distinct fluorescence images (DAPI and Texas Red or DAPI and FITC) were obtained from each slide and were merged via Axiovision LE software (Carl Zeiss, Germany). From this merged image, I localized specific antigens in the capsular tissue around the implant. For macrophages, I counted all of the cells in the image.

4.3 Results

4.3.1 Number of M1 and M2 macrophages

IF staining was performed to investigate changes in macrophage phenotype. M1 and M2 macrophages were separated and analyzed. M1 macrophages were observed to be dominant in all the groups, and the number of M1 macrophages in the PLGA_MON_SI and MON_SI groups loaded with drugs was observed to be small. This tendency lasted for up to 2 weeks, but after 4 weeks, the results of the MON_SI group were similar to those of the drug-free group. In the PLGA_MON_SI group, the number of M1 macrophages was observed to be less than that at 12 weeks. M1 macrophages were highly expressed at the early stage of transplantation, and then gradually decreased over time. (Fig. 4.1 and Fig. 4.2(a))

In the case of M2 macrophages, a higher number of M2 macrophages was observed when the drug was loaded, and this tendency was confirmed for up to 12 weeks. Specifically, in the PLGA_MON_SI group, the number of M2 macrophages was significantly higher than in the SI group at 4 and 12 weeks. In the case of M2 macrophages, a tendency to increase gradually was observed. (Fig. 4.1 and Fig. 4.2(b))

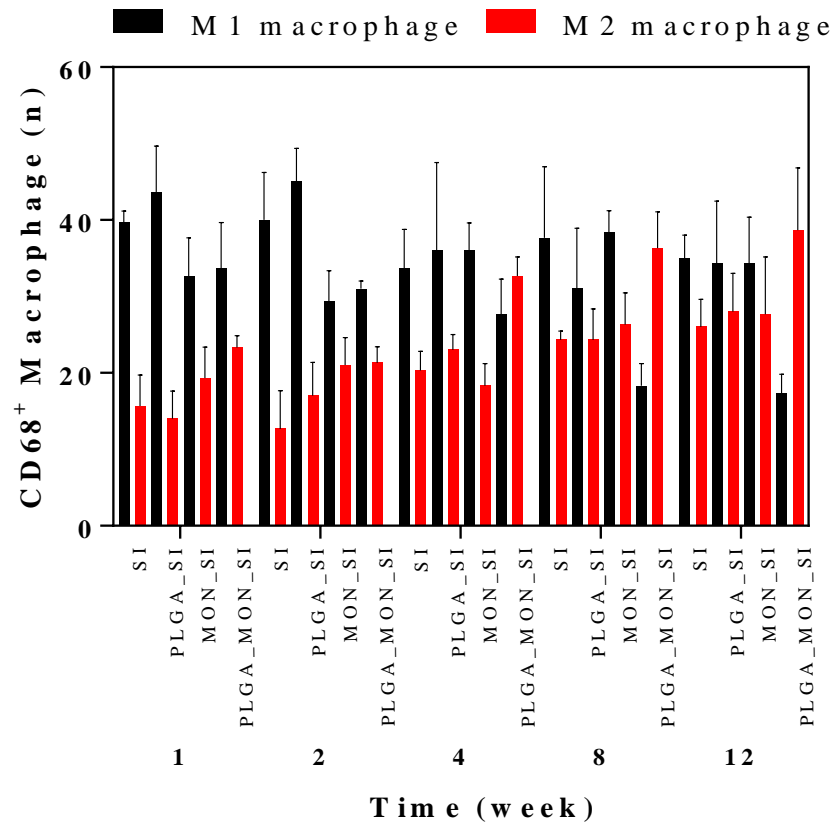


Figure 4.1 Total number of macrophages

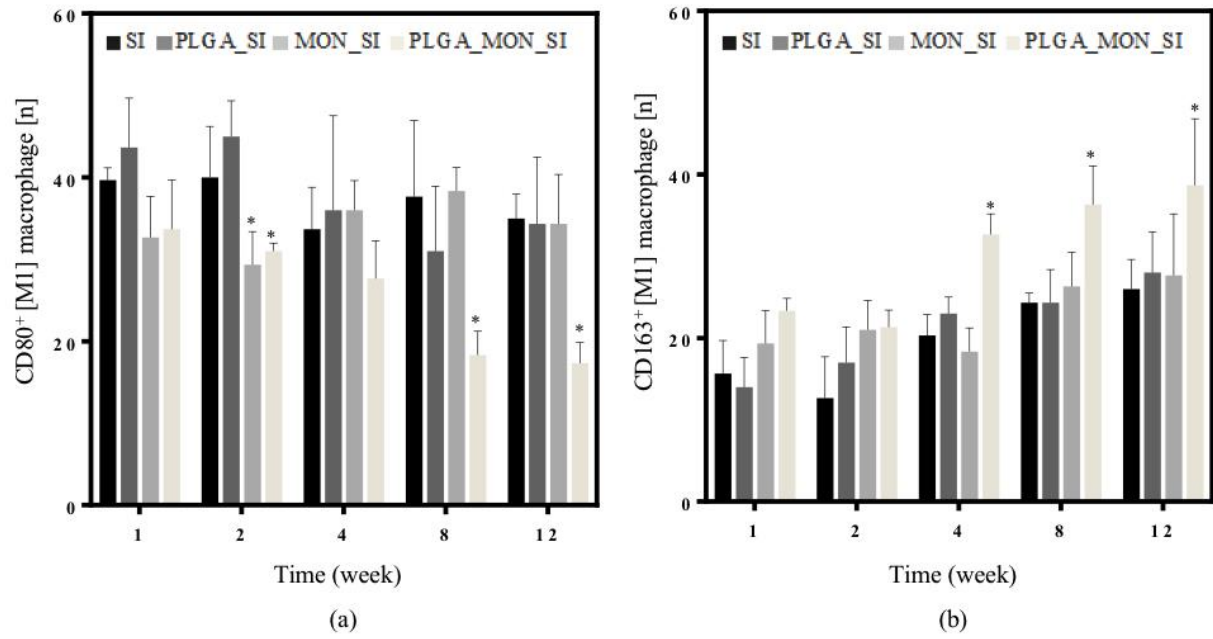


Figure 4.2 Number of M1 and M2 macrophages (a) Profile of M1 macrophages, and (b) profile of M2 macrophages

4.3.2 M1 and M2 macrophage ratio analysis

At week 1, the proportion of M1/M2 macrophages was higher in the non-drug-loaded groups (SI and PLGA_SI) than in the two drug-loaded groups (MON_SI and PLGA_MON_SI). This tendency was maintained for up to 2 weeks, and at week 4, similar values were observed in all the groups except for the PLGA_MON_SI group. The PLGA_MON_SI group had the lowest value for up to 12 weeks, and the MON_SI group had a value similar to that of the non-drug-loaded group at week 4. The M1/M2 ratio tended to decrease steadily over time.

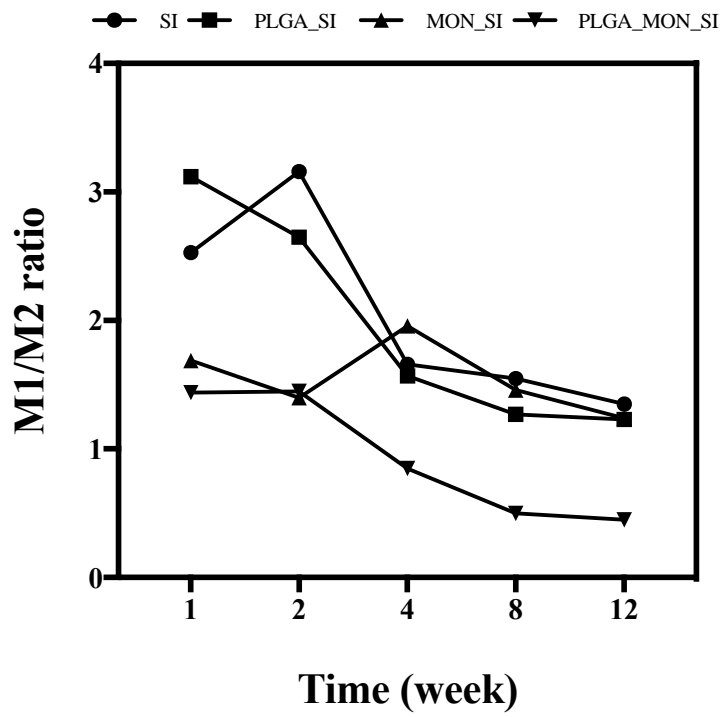


Figure 4.3 M1/M2 ratio

Table 4.1 M1/M2 ratio analysis

M1/M2 ratio	SI	PLGA_SI	MON_SI	PLGA_MON_SI
Week 1	2.53	3.12	1.69	1.44
Week 2	3.16	2.65	1.40	1.45
Week 4	1.66	1.57	1.96	0.85
Week 8	1.55	1.27	1.46	0.50
Week 12	1.35	1.23	1.24	0.45

4.4 Discussion

Fibrosis generated by implantable medical devices occurs continuously through multistep active reactions. Therefore, an analysis of various fibrosis-related factors is needed, and the need for studies aimed at inhibiting fibrosis based on the expression pattern of these factors will increase. Based on the results described in Chapters 2 and 3 of this study, I confirmed the inhibitory effect of montelukast on *in vivo* fibrosis. However, there was no significant difference in the number of macrophages, and thus, an additional analysis of the effect of macrophage phenotype was performed.

Macrophages are divided into two phenotypes (i.e., M1 and M2), and each phenotype is expressed at a certain time and exerts a different effect [95]. M1 macrophages are known to play a leading role in the initial inflammation reaction, and M2 macrophages terminate the inflammatory reaction in the late inflammation period via IL-10 [97]. Analysis of the results of this study showed that treatment with montelukast tended to decrease the number of M1 macrophages in the initial phase of inflammation, which leads to inhibition of the inflammatory response caused by M1 macrophages via secretion of IL-1 and IL-6. Based on these facts, a fibrosis inhibitory effect can be predicted due to the decrease in M1 macrophages. In the case of M2 macrophages, a relatively large number was observed in the PLGA_MON_SI group during the initial inflammatory reaction, which suggests that the inflammatory reaction was prematurely terminated by M2 macrophages, thereby suppressing the inflammatory amplification reaction mediated by M1 regulation and activating the fibrotic phase.

Based on these results, I confirmed that the macrophage phenotype was altered by treatment with the drug montelukast, which decreased the number of M1 macrophages in the initial inflammation phase and increased the number of M2 macrophages, leading to suppression of the inflammatory response.

4.5 Conclusion

In this study, I investigated the mechanisms associated with fibrosis inhibition *in vivo* and examined the possibility of inhibiting fibrosis with montelukast. Based on the results of this study, I confirmed that montelukast regulates the activity of M1 macrophages, increases the number of M2 macrophages, inhibits inflammation, and regulates fibrosis through early termination of inflammatory mechanisms.

Chapter 5

Conclusion and Perspectives

Fibrosis has occurred since the beginning of the implantable medical device market, and various approaches have been applied to solve the problem of fibrosis associated with these devices. Breast implants are intended to avoid the occurrence of fibrosis through modification of the shell surface, and other implantable medical devices have been developed with the aim of ensuring and maximizing the safety of these biomaterials. However, despite these developments, modern implantable medical devices still do not prevent fibrosis. In the long term, this side effect not only leads to patient discomfort but also causes other life-threatening issues, such as reduction of the lifespan of functional implantable medical devices (e.g., defibrillators and pacemakers) and decreasing functionality. Thus, fibrosis in response to implantable medical devices is a problem that needs to be solved, and further research is needed. In this study, I tried to find a new drug that can suppress fibrosis caused by silicone implants and screened the general steps of fibrosis that can occur when silicone materials are implanted. In addition, I also recommended new drugs and examined the possibility of using these drugs as suppressors of the fibrosis mechanism. In Chapter 2, I evaluated the general stages of fibrosis associated with silicone implants and obtained information about the

expression pattern of the major factors involved in the fibrosis pathway. First, the inflammatory responses were increased at the early phase of implantation, and several fibrosis factors (i.e., TGF- β , fibroblasts and myofibroblasts) were activated and recruited as a result of the inflammatory reaction. Each factor showed a tendency to increase over time. Finally, I confirmed once again that fibrosis occurs due to a chain reaction involving the factors mentioned in Chapter 2.

In this study, the fibrosis pathway was reconstructed based on previous studies. For the first time, I showed that the inflammatory response begins concomitantly with the recruitment of PMNs. PMNs release various inflammatory factors (IL-1, IL-6, IL-17 and IL-23) and leukotrienes into the periphery of the silicone implants. These inflammatory mediators play different roles. IL-1 and IL-6 recruit macrophages to the periphery of the tissue and cause a change in the phenotype of “classically activated” (M1) macrophages. Leukotrienes, which are secreted by PMNs, maintain the activity of the inflammatory cells through autocrine and paracrine effects, and at the same time further maintain and amplify the inflammatory response by recruiting inflammatory cells (PMNs). This activity is predominant in the acute inflammatory stage, and during the progression to chronic inflammation, the number of “alternatively activated” M2 macrophages increases along with an increase in IL-17 activity, and the inflammatory response is regulated via this mechanism. These phenotypic changes occur throughout the fibrosis period, with M2 macrophages predominating as inflammation progress to the later stages. Changes in these phenotypes regulate the inflammatory response, thereby ending the inflammatory response. After the inflammation phase, the expression of TGF- β is predominantly caused by the activity of macrophages and fibroblasts. The resulting TGF- β promotes fibroblast activation and leukotriene secretion, which typically occur in the inflammation phase. Leukotriene and TGF- β induce collagen synthesis at the periphery of the implants through induction of fibroblast activity, and TGF- β specifically induces differentiation and activation of fibroblasts to myofibroblasts. This overall process increases collagen synthesis at the periphery of the implant due to the activity of TGF- β and leukotriene. Finally, these phenomena terminate the fibrosis process by

isolating the implanted silicone implants from the interior of the body.

Based on the results described in Chapter 3 and Chapter 4, I demonstrated that inhibition of fibrosis is possible via leukotriene regulation by montelukast. Oral montelukast administration is common, and the bioavailability is approximately 64 % in the human body. The generally recommended dosage is 10 mg to 2 g once a day. In this study, the montelukast dose was converted to blood concentration, and the concentration was determined based on the pharmacokinetics (64 % bioavailability). Assuming that 6.4 to 1,280 mg of montelukast is dissolved in 5 L of blood (human adult blood volume), the concentration of the drug in the blood is 1.28 to 256 $\mu\text{g/ml}$. The concentration of montelukast used in this study was $177.31 \pm 6.77 \mu\text{g}$ in the MON_SI group and $276.31 \pm 7.63 \mu\text{g}$ in the PLGA_MON_SI group. Based on this information, it was estimated that montelukast at a concentration of approximately 6.82 to 10.63 $\mu\text{g/ml}$ was delivered to the rat blood and therefore was well within the effective dose of montelukast (1.28 ~ 256 $\mu\text{g/ml}$).

Leukotrienes are expressed by inflammatory cells (PMNs) and increase PMN accumulation via an autocrine effect. However, in the MON_SI and PLGA_MON_SI groups in which montelukast was administered, the number of PMNs in the inflammation phase was reduced by a leukotriene suppression effect (Fig. 3.6). This tendency was observed only in the drug-loading group (MON_SI and PLGA_MON_SI) in the first two weeks, and the inflammation throughout the entire experimental period was decreased in the long-term drug delivery group (PLGA_MON_SI) until week 12. This effect was predicted to regulate the activity of leukotrienes throughout the entire inflammation phase (acute and chronic inflammation) only if the drug was delivered by day 15. Second, I analyzed the number of macrophages in the inflammation phase and the late foreign body reaction phase and confirmed that the number of macrophages was not different in each group at each time point (Fig. 3.7). However, a specific difference in macrophage phenotype was observed (Fig. 4.1 and 4.2), confirming that M1 macrophage expression was lower in the drug-loaded groups. This decrease in M1 macrophage number was found to regulate the inflammatory response amplified by early M1

macrophages, and the increase in M2 macrophages in the drug-loaded group was predicted to regulate the inflammatory response once again. This M2 macrophage predominant ratio was confirmed to persist for up to 12 weeks in the drug-loaded group treated for 15 days (Fig. 4.3). Ultimately, these regulatory phenomena suppressed the inflammation phase in the fibrosis reaction and regulated the activity of fibroblasts, finally suppressing fibrosis. Third, the TGF- β expression levels were examined, and the expression pattern of TGF- β was found to be similar to that of the overall inflammation tendency (Fig. 3.6). This finding was predicted by a decrease in the expression level of TGF- β due to a reduction in the inflammatory response, and this tendency was also observed to affect the number of late fibroblasts and myofibroblasts (Fig. 3.8 and 3.9). In the PLGA_MON_SI group, in which the drug was delivered for more than 15 days, the number of fibroblasts and myofibroblasts showed a tendency to decrease by week 12. This tendency was also observed in the final capsule thickness and collagen density. In summary, montelukast regulates the activity of leukotrienes expressed by early PMNs and regulates the expression of IL-1, IL-6, IL-17 and IL-23. These effects alter the number of PMNs and the macrophage phenotype ratio (Fig. 4.3). Changes in the phenotype of these macrophages suppress the inflammatory response by regulating the expression of pro-inflammatory cytokines and reducing the number of M1 macrophages in the inflammation phase. Suppression of the inflammatory phase by leukotrienes plays an important role in the activity and number of fibroblasts and myofibroblasts as well as in control of the TGF- β expression level. In addition, leukotrienes released during the inflammatory stage suppress collagen synthesis and capsule formation through additional regulatory effects on fibroblasts and myofibroblasts during the foreign body reaction phase. Based on these results, montelukast, which has been used as a conventional asthma medication, was confirmed to suppress leukotrienes *in vivo* by controlling the overall fibrosis pathway, thus regulating fibrosis. Therefore, montelukast may be applied as a novel fibrosis suppressor.

Future implantable medical devices will continue to develop and will evolve as needed. In

addition, their form and function will continue to evolve according to various needs. However, unless there is an improvement in the materials and safety is ensured, adverse fibrosis effects will continuously follow these materials. In the future implantable medical device market, it will be necessary to secure both function and safety and to maintain safety without any side effects *in vivo*. From this aspect, in this study, it was important to verify the steps based on fibrosis that occurred most frequently to identify a new drug that can suppress fibrosis. Further research and fibrosis analyses are required to aid in the development of future implantable medical devices.

References

- [1] B.R. Burkhardt, Capsular contracture: hard breasts, soft data, *Clinics in plastic surgery* 15(4) (1988) 521–532.
- [2] A. Araco, R. Caruso, F. Araco, J. Overton, G. Gravante, Capsular contractures: a systematic review, *Plast. Reconstr. Surg.* 124(6) (2009) 1808–1819.
- [3] J.H. Rosing, G. Wong, M.S. Wong, D. Sahar, T.R. Stevenson, L.L. Pu, Autologous fat grafting for primary breast augmentation: a systematic review, *Aesthetic plastic surgery* 35(5) (2011) 882–890.
- [4] C.-H. Wong, M. Samuel, B.-K. Tan, C. Song, Capsular contracture in subglandular breast augmentation with textured versus smooth breast implants: a systematic review, *Plastic and reconstructive surgery* 118(5) (2006) 1224–1236.
- [5] A.J. Bridges, F.B. Vasey, Silicone breast implants: history, safety, and potential complications, *Archives of internal medicine* 153(23) (1993) 2638–2644.
- [6] T.W. Uroskie Jr, L.B. Colen, History of breast reconstruction, *Seminars in plastic surgery*, Thieme Medical Publishers, 2004, p. 65.
- [7] J.M. Anderson, A. Rodriguez, D.T. Chang, Foreign body reaction to biomaterials, *Semin. Immunol.* 20(2) (2008) 86.
- [8] G. Wick, C. Grundtman, C. Mayerl, T.-F. Wimpissinger, J. Feichtinger, B. Zelger, R. Sgonc, D. Wolfram, The immunology of fibrosis, *Annual review of immunology* 31 (2013) 107–135.
- [9] P.H. Zeplin, A. Larena-Avellaneda, K. Schmidt, Surface modification of silicone breast implants by binding the antifibrotic drug halofuginone reduces capsular fibrosis, *Plast. Reconstr. Surg.* 126(1) (2010) 266–274.
- [10] N. Handel, J.A. Jensen, Q. Black, J.R. Waisman, M.J. Silverstein, The fate of breast implants: a critical analysis of complications and outcomes, *Plast. Reconstr. Surg.* 96(7) (1995) 1521.
- [11] L. Tang, J.W. Eaton, Inflammatory responses to biomaterials, *American journal of clinical pathology* 103(4) (1995) 466–471.
- [12] G.B. Ryan, G. Majno, Acute inflammation. A review, *The American journal of pathology* 86(1)

(1977) 183.

[13] N. Khalil, O. Bereznay, M. Sporn, A. Greenberg, Macrophage production of transforming growth factor beta and fibroblast collagen synthesis in chronic pulmonary inflammation, *J. Exp. Med.* 170(3) (1989) 727–737.

[14] A.B. Roberts, M.B. Sporn, Transforming growth factor- β , *The molecular and cellular biology of wound repair*, Springer 1988, pp. 275–308.

[15] H. Headon, A. Kasem, K. Mokbel, Capsular contracture after breast augmentation: an update for clinical practice, *Archives of plastic surgery* 42(5) (2015) 532.

[16] G.R. Tintinger, C. Feldman, A.J. Theron, R. Anderson, Montelukast: more than a cysteinyl leukotriene receptor antagonist?, *ScientificWorldJournal* 10 (2010) 2403–2413.

[17] Y. Kanaoka, J.A. Boyce, Cysteinyl leukotrienes and their receptors: cellular distribution and function in immune and inflammatory responses, *The Journal of Immunology* 173(3) (2004) 1503–1510.

[18] B.J. Lipworth, Leukotriene-receptor antagonists, *The Lancet* 353(9146) (1999) 57–62.

[19] T. Jones, M. Labelle, M. Belley, E. Champion, L. Charette, J. Evans, A. Ford-Hutchinson, J.-Y. Gauthier, A. Lord, P. Masson, Pharmacology of montelukast sodium (Singular[™]), a potent and selective leukotriene D₄ receptor antagonist, *Can. J. Physiol. Pharm.* 73(2) (1995) 191–201.

[20] F. Engels, F. Nijkamp, Pharmacological inhibition of leukotriene actions, *Pharmacy World and Science* 20(2) (1998) 60–65.

[21] C.D. Funk, Prostaglandins and leukotrienes: advances in eicosanoid biology, *science* 294(5548) (2001) 1871–1875.

[22] T.C. Beller, D.S. Friend, A. Maekawa, B.K. Lam, K.F. Austen, Y. Kanaoka, Cysteinyl leukotriene 1 receptor controls the severity of chronic pulmonary inflammation and fibrosis, *Proceedings of the National Academy of Sciences of the United States of America* 101(9) (2004) 3047–3052.

[23] R. Eap, E. Jacques, A. Semlali, S. Plante, J. Chakir, Cysteinyl leukotrienes regulate TGF- β 1 and collagen production by bronchial fibroblasts obtained from asthmatic subjects, *Prostaglandins Leukot. Essent. Fatty Acids* 86(3) (2012) 127–133.

[24] S. Takayanagi, Complication of breast implant, *J. Jpn. Soc. Aesthet. Plast. Surg.* 28(4) (2006)

180–185.

- [25] S.E. Gabriel, J.E. Woods, W.M. O'Fallon, C.M. Beard, L.T. Kurland, L.J. Melton, Complications leading to surgery after breast implantation, *N. Engl. J. Med.* 336(10) (1997) 677–682.
- [26] D.T. Luttikhuisen, M.C. Harmsen, M.J.V. Luyn, Cellular and molecular dynamics in the foreign body reaction, *Tissue engineering* 12(7) (2006) 1955–1970.
- [27] R. Klopffleisch, F. Jung, The pathology of the foreign body reaction against biomaterials, *Journal of Biomedical Materials Research Part A* 105(3) (2017) 927–940.
- [28] W. Siggelkow, A. Faridi, K. Spiritus, U. Klinge, W. Rath, B. Klosterhalfen, Histological analysis of silicone breast implant capsules and correlation with capsular contracture, *Biomaterials* 24(6) (2003) 1101–1109.
- [29] B. Rolfe, J. Mooney, B. Zhang, S. Jahnke, S.-J. Le, Y.-Q. Chau, Q. Huang, H. Wang, G. Campbell, J. Campbell, The fibrotic response to implanted biomaterials: implications for tissue engineering, *Regenerative Medicine and Tissue Engineering—Cells and Biomaterials*, InTech2011.
- [30] D.F. Williams, On the nature of biomaterials, *Biomaterials* 30(30) (2009) 5897–5909.
- [31] L. Zhang, Z. Cao, T. Bai, L. Carr, J.-R. Ella-Menye, C. Irvin, B.D. Ratner, S. Jiang, Zwitterionic hydrogels implanted in mice resist the foreign-body reaction, *Nature biotechnology* 31(6) (2013) 553.
- [32] I.A. Darby, T.D. Hewitson, Fibroblast differentiation in wound healing and fibrosis, *Int. Rev. Cytol.* 257 (2007) 143–179.
- [33] W. Roche, Fibroblasts and fibrosis, *Clin. Exp. Allergy* 21(5) (1991) 635–636.
- [34] C.A. Feghali, T.M. Wright, Cytokines in acute and chronic inflammation, *Front Biosci* 2(1) (1997) d12–d26.
- [35] J.-M. Zhang, J. An, Cytokines, inflammation and pain, *International anesthesiology clinics* 45(2) (2007) 27.
- [36] S.R. Beanes, C. Dang, C. Soo, K. Ting, Skin repair and scar formation: the central role of TGF- β , *Expert reviews in molecular medicine* 5(8) (2003) 1–22.
- [37] A. Leask, D.J. Abraham, TGF- β signaling and the fibrotic response, *The FASEB Journal* 18(7) (2004) 816–827.
- [38] D.A. De Albuquerque, V. Saxena, D.E. Adams, G.P. Boivin, H.I. Brunner, D.P. Witte, R.R. Singh,

An ACE inhibitor reduces Th2 cytokines and TGF- β 1 and TGF- β 2 isoforms in murine lupus nephritis, *Kidney international* 65(3) (2004) 846–859.

[39] D. Baeten, P. Demetter, C.A. Cuvelier, E. Kruithof, N. Van Damme, M. De Vos, E.M. Veys, F. De Keyser, Macrophages expressing the scavenger receptor CD163: a link between immune alterations of the gut and synovial inflammation in spondyloarthritis, *The Journal of pathology* 196(3) (2002) 343–350.

[40] W. Dolores, R. Christian, N. Harald, P. Hildegunde, W. Georg, Cellular and molecular composition of fibrous capsules formed around silicone breast implants with special focus on local immune reactions, *J. Autoimmun.* 23(1) (2004) 81–91.

[41] S.L. Spear, P.M. Parikh, J.A. Goldstein, History of breast implants and the Food and Drug Administration, *Clin. Plast. Surg.* 36(1) (2009) 15–21.

[42] M.C. Champaneria, W.W. Wong, M.E. Hill, S.C. Gupta, The evolution of breast reconstruction: a historical perspective, *World J. Surg.* 36(4) (2012) 730–742.

[43] S. Bondurant, V. Ernster, R. Herdman, Institute of Medicine (U.S.). Committee on the Safety of Silicone Breast Implants, *Safety of Silicone Breast Implants*, National Academy Press, Washington, DC, 2000.

[44] A.O. Momoh, R. Ahmed, B.P. Kelley, O. Aliu, K.M. Kidwell, J.H. Kozlow, K.C. Chung, A systematic review of complications of implant-based breast reconstruction with prereconstruction and postreconstruction radiotherapy, *Ann. Surg. Oncol.* 21(1) (2014) 118–24.

[45] T.A. Wynn, T.R. Ramalingam, Mechanisms of fibrosis: therapeutic translation for fibrotic disease, *Nat. Med.* 18(7) (2012) 1028–1040.

[46] K.S. Jones, Effects of biomaterial-induced inflammation on fibrosis and rejection, *Semin. Immunol.* 20(2) (2008) 130–136.

[47] J.M. Anderson, Mechanisms of inflammation and infection with implanted devices, *Cardiovasc. Pathol.* 2(3) (1993) 33–41.

[48] M. Peters-Golden, W.R. Henderson Jr, Leukotrienes, *N. Engl. J. Med.* 357(18) (2007) 1841–1854.

[49] W. Busse, M. Kraft, Cysteinyl Leukotrienes in Allergic Inflammation Strategic Target for Therapy,

CHEST 127(4) (2005) 1312–1326.

[50] D.J. Figueroa, R.M. Breyer, S.K. Defoe, S. Kargman, B.L. Daugherty, K. Waldburger, Q. Liu, M. Clements, Z. Zeng, G.P. O'Neill, T.R. Jones, K.R. Lynch, C.P. Austin, J.F. Evans, Expression of the cysteinyl leukotriene 1 receptor in normal human lung and peripheral blood leukocytes, *Am. J. Respir. Crit. Care Med.* 163(1) (2001) 226–33.

[51] L. Baud, J. Perez, M. Denis, R. Ardaillou, Modulation of fibroblast proliferation by sulfidopeptide leukotrienes: effect of indomethacin, *J. Immunol.* 138(4) (1987) 1190–1195.

[52] G.S. Ashcroft, Bidirectional regulation of macrophage function by TGF- β , *Microbes Infect.* 1(15) (1999) 1275–1282.

[53] S.M. Wahl, Transforming growth factor beta (TGF- β) in inflammation: a cause and a cure, *J. Clin. Immunol.* 12(2) (1992) 61–74.

[54] D. Danielpour, L.L. Dart, K.C. Flanders, A.B. Roberts, M.B. Sporn, Immunodetection and quantitation of the two forms of transforming growth factor-beta (TGF- β 1 and TGF- β 2) secreted by cells in culture, *J. Cell. Physiol.* 138(1) (1989) 79–86.

[55] B. Hinz, Formation and function of the myofibroblast during tissue repair, *J. Invest. Dermatol.* 127(3) (2007) 526–537.

[56] A.R. Gasset, C.H. Dohlman, The tensile strength of corneal wounds, *Arch. Ophthalmol.* 79(5) (1968) 595–602.

[57] M. Peters–Golden, M.M. Gleason, A. Togias, Cysteinyl leukotrienes: multi–functional mediators in allergic rhinitis, *Clin. Exp. Allergy* 36(6) (2006) 689–703.

[58] T. Asakura, Y. Ishii, K. Chibana, T. Fukuda, Leukotriene D4 stimulates collagen production from myofibroblasts transformed by TGF- β , *J. Allergy Clin. Immunol.* 114(2) (2004) 310–315.

[59] M.J. Gizycki, E. Adelroth, A.V. Rogers, P.M. O'Byrne, P.K. Jeffery, Myofibroblast involvement in the allergen–induced late response in mild atopic asthma, *Am. J. Respir. Cell Mol. Biol.* 16(6) (1997) 664–73.

[60] A.M. Vignola, F. Mirabella, G. Costanzo, R. Di Giorgi, M. Gjomarkaj, V. Bellia, G. Bonsignore, Airway remodeling in asthma, *CHEST* 123(3_suppl) (2003) 417S–422S.

[61] T.L. Smith, N.B. Sautter, Is montelukast indicated for treatment of chronic rhinosinusitis with

- polyposis?, *Laryngoscope* 124(8) (2014) 1735–1736.
- [62] J.W. Steinke, J.L. Kennedy, Leukotriene inhibitors in sinusitis, *Curr. Infect. Dis. Rep.* 14(2) (2012) 147–154.
- [63] J. Kato, T. Kohyama, H. Okazaki, M. Desaki, T. Nagase, S.I. Rennard, H. Takizawa, Leukotriene D4 potentiates fibronectin-induced migration of human lung fibroblasts, *Clin. Immunol.* 117(2) (2005) 177–181.
- [64] S. Freiberg, X. Zhu, Polymer microspheres for controlled drug release, *Int. J. Pharm.* 282(1–2) (2004) 1–18.
- [65] C. Shasteen, Y.B. Choy, Controlling degradation rate of poly (lactic acid) for its biomedical applications, *Biomed. Eng. Lett.* 1(3) (2011) 163–167.
- [66] A. Spano, B. Palmieri, T. Palmizi Taidelli, M. Nava, Reduction of capsular thickness around silicone breast implants by zafirlukast in rats, *European Surgical Research* 41(1) (2008) 8–14.
- [67] M. Moreira, D.J. Fagundes, M. de Jesus Simões, M.C.B.M. de Oliveira, I.T. dos Santos Previdelli, A.C. Moreira, Zafirlukast pocket delivery impairs the capsule healing around textured implants in rats, *Aesthetic plastic surgery* 33(1) (2009) 90–97.
- [68] S.H. Kang, K.C. Shin, W.S. Kim, T.H. Bae, H.K. Kim, M.K. Kim, The Preventive Effect of Topical Zafirlukast Instillation for Peri-Implant Capsule Formation in Rabbits, *Archives of plastic surgery* 42(2) (2015) 179–185.
- [69] S. Park, M. Park, B.H. Kim, J.E. Lee, H.J. Park, S.H. Lee, C.G. Park, M.H. Kim, R. Kim, E.H. Kim, Acute suppression of TGF- β with local, sustained release of tranilast against the formation of fibrous capsules around silicone implants, *J. Control. Release* 200 (2015) 125–137.
- [70] R. Ruiz-de-Erenchun, J.D. de las Herrerías, B. Hontanilla, Use of the transforming growth factor- β 1 inhibitor peptide in periprosthetic capsular fibrosis: experimental model with tetraglycerol dipalmitate, *Plast. Reconstr. Surg.* 116(5) (2005) 1370–1378.
- [71] P. Nair, H. Duncan, T. Pitt Ford, H. Luder, Histological, ultrastructural and quantitative investigations on the response of healthy human pulps to experimental capping with mineral trioxide aggregate: a randomized controlled trial, *Int. Endod. J.* 41(2) (2008) 128–150.
- [72] M.R. Ward, P. Kanellakis, D. Ramsey, J. Funder, A. Bobik, Eplerenone suppresses constrictive

remodeling and collagen accumulation after angioplasty in porcine coronary arteries, *Circulation* 104(4) (2001) 467–472.

[73] R. McMullen, E. Bauza, C. Gondran, G. Oberto, N. Domloge, C.D. Farra, D. Moore, Image analysis to quantify histological and immunofluorescent staining of ex vivo skin and skin cell cultures, *Int. J. Cosmet. Sci.* 32(2) (2010) 143–154.

[74] D.L. Pavia, G.M. Lampman, G.S. Kriz, J.R. Vyvyan, *Introduction to Spectroscopy*, Brooks/Cole, Belmont, CA, 2009.

[75] T. Paragkumar N, D. Edith, J.-L. Six, Surface characteristics of PLA and PLGA films, *Appl. Surf. Sci.* 253(5) (2006) 2758–2764.

[76] H. Lodish, A. Berk, S.L. Zipursky, P. Matsudaira, D. Baltimore, J. Darnell, *Molecular Cell Biology*, W.H. Freeman, New York, 2000.

[77] G.R. Grotendorst, Connective tissue growth factor: a mediator of TGF- β action on fibroblasts, *Cytokine Growth Factor. Rev.* 8(3) (1997) 171–179.

[78] A. Leask, D.J. Abraham, TGF- β signaling and the fibrotic response, *FASEB J.* 18(7) (2004) 816–827.

[79] G.J. Prud'homme, Pathobiology of transforming growth factor β in cancer, fibrosis and immunologic disease, and therapeutic considerations, *Lab. Invest.* 87(11) (2007) 1077–1091.

[80] K. Hwang, H.B. Sim, F. Huan, D.J. Kim, Myofibroblasts and capsular tissue tension in breast capsular contracture, *Aesthetic Plast. Surg.* 34(6) (2010) 716–721.

[81] L. Tang, T.A. Jennings, J.W. Eaton, Mast cells mediate acute inflammatory responses to implanted biomaterials, *Proceedings of the National Academy of Sciences* 95(15) (1998) 8841–8846.

[82] M. Avula, A. Rao, L. McGill, D.W. Grainger, F. Solzbacher, Foreign body response to subcutaneous biomaterial implants in a mast cell-deficient Kitw-Sh murine model, *Acta biomaterialia* 10(5) (2014) 1856–1863.

[83] S. Orenstein, E. Saberski, U. Klueh, D. Kreutzer, Y. Novitsky, Effects of mast cell modulation on early host response to implanted synthetic meshes, *Hernia* 14(5) (2010) 511–516.

[84] M. Peters-Golden, W.R. Henderson Jr, Leukotrienes, *New England Journal of Medicine* 357(18) (2007) 1841–1854.

- [85] R.A. Evans, Y.C. Tian, R. Steadman, A.O. Phillips, TGF- β 1-mediated fibroblast-myofibroblast terminal differentiation—the role of smad proteins, *Exp. Cell Res.* 282(2) (2003) 90–100.
- [86] C.K. Huang, N. Handel, Effects of Singulair (montelukast) treatment for capsular contracture, *Aesthet. Surg. J.* 30(3) (2010) 404–408.
- [87] N. Scuderi, M. Mazzocchi, P. Fioramonti, G. Bistoni, The effects of zafirlukast on capsular contracture: preliminary report, *Aesthetic Plast. Surg.* 30(5) (2006) 513–20.
- [88] D. Price, Tolerability of montelukast, *Drugs* 59(1) (2000) 35–42.
- [89] G. Catanuto, A. Spano, A. Pennati, E. Riggio, G. Farinella, G. Impoco, S. Spoto, G. Gallo, M. Nava, Experimental methodology for digital breast shape analysis and objective surgical outcome evaluation, *J. Plast. Reconstr. Aesthet. Surg.* 61(3) (2008) 314–318.
- [90] K. Priyanka, S.A. Abdul Hasan, Preparation and evaluation of montelukast sodium loaded solid lipid nanoparticles, *J. Young Pharm.* 4(3) (2012) 129–137.
- [91] E. Bettelli, Y. Carrier, W. Gao, T. Korn, T.B. Strom, M. Oukka, H.L. Weiner, V.K. Kuchroo, Reciprocal developmental pathways for the generation of pathogenic effector T H 17 and regulatory T cells, *Nature* 441(7090) (2006) 235.
- [92] M. Veldhoen, R.J. Hocking, C.J. Atkins, R.M. Locksley, B. Stockinger, TGF β in the context of an inflammatory cytokine milieu supports de novo differentiation of IL-17-producing T cells, *Immunity* 24(2) (2006) 179–189.
- [93] C.L. Langrish, Y. Chen, W.M. Blumenschein, J. Mattson, B. Basham, J.D. Sedgwick, T. McClanahan, R.A. Kastelein, D.J. Cua, IL-23 drives a pathogenic T cell population that induces autoimmune inflammation, *Journal of Experimental Medicine* 201(2) (2005) 233–240.
- [94] J.K. Kolls, A. Lindén, Interleukin-17 family members and inflammation, *Immunity* 21(4) (2004) 467–476.
- [95] D.M. Mosser, J.P. Edwards, Exploring the full spectrum of macrophage activation, *Nature reviews immunology* 8(12) (2008) 958.
- [96] A. Cordeiro-da-Silva, J. Tavares, N. Araújo, F. Cerqueira, A. Tomás, P.K.T. Lin, A. Ouaiissi, Immunological alterations induced by polyamine derivatives on murine splenocytes and human

mononuclear cells, *International immunopharmacology* 4(4) (2004) 547–556.

[97] S. Gordon, Alternative activation of macrophages, *Nature reviews immunology* 3(1) (2003) 23.

Abstract in Korean

1. 국문요약

실리콘 재질의 이식형 의료기기는 그 쓰임새에 따라 다양한 형태를 지니고 발전해 왔다. 하지만 이러한 실리콘 보형물의 경우 생체 내 이식 시 발생하는 부작용으로 인해 그 쓰임의 한계점이 존재하고 있는 실정이다. 이러한 실리콘 재질의 이식형 의료기기 중에도 실리콘 유방 보형물에서 많은 부작용이 보고되고 있는 실정이다. 대표적인 부작용으로 구형 구축이 존재하고 있으며, 생체 내 면역 반응으로 인해 매개되고 심한 경우 환자에게 2차 적인 수술을 요구할 뿐만 아니라, 통증을 야기한다. 이러한 관점에서 실리콘 유방 보형물의 삽입 시 발생 가능한 부작용의 발생 단계를 이해하고, 이를 기반으로 섬유화 부작용을 억제하는 것은 앞으로의 보형물 개발에 주요한 관심사가 될 것이다.

본 연구에서는 이러한 관점에서 생체 내 이식된 실리콘 보형물의 섬유화 발생 단계를 검증하고, 이를 기반으로 섬유화 억제를 위한 약물의 제어 전달을 통해 섬유화 부작용을 억제하고자 하였으며, 대식세포의 발현 양상을 분석함으로써 섬유화 부작용 억제 기작에서의 전반적인 프로세스를 검증하고 효과적인 섬유화 억제 기능을 지닌 섬유화 억제 보형물을 개발함과 동시에, 몬테루카스트라는 새로운 약물의 도입을 통해 기존의 약물 효능 뿐만 아니라 섬유화 단계에서의 억제 효과 약물 적용 가능 여부를 검증하였다. 먼저 조직에서의 섬유화 반응 단계의 인자 검증을 위해 2cm 지름의 실리콘 보형물의 Shell을 제작하였으며, 약물 탑재를 위한 공정을 도입한 후, 이를 의료용 접합제를 이용하여 접합하여 약물 탑재 표면이 양면으로 드러나도록 처리하였다. 각기 다른 4개의 그룹의 샘플을 제작하였고, 이를 8주령 Sprague-Dawley Rat 등 부위 피하조직층에 이식을 하였으며, 총 5번의 정해진 이식 기간(1, 2, 4, 8, 12주) 에 따라 생검하여 섬유화 반응 단계별 인자 억제 유무를 검증하고자 하였다. 가설에 따라 섬유화 관련 인자인 7개의 인자(염증반응, 대식세포, 섬유아세포, 형질전환성장인자-베타, 근육섬유모세포, 교원섬유밀도,

섬유막두께를 대상으로 이식 기간 별 생체 내 발현 양상에 대해 검증하였으며, 염증 반응의 경우에는 초기 SI, PLGA_SI 그룹에서 높은 발현 양상을 보이나, 약물이 탑재된 MON_SI, PLGA_MON_SI 그룹의 경우 발현 양상이 감소되는 것으로 확인되었다. 섬유화 연관 인자들의 경우 SI, PLGA_SI 그룹에서 지속적인 증가 경향성이 관찰되었으며, 특이적으로 약물이 단기간 전달되는 MON_SI 그룹에서는 4주까지 낮은 수치의 발현 양상을 보이다 8주 이후부터 증가 경향이 관찰되었으며, 12주에는 약물이 탑재되지 않은 그룹과 동일한 수치의 결과가 관찰되었다. PLGA_MON_SI 그룹의 경우에는 모든 섬유화 관련 인자들이 12주까지 억제 되는 경향성을 보였으며, 최종적으로 몬테루카스트 약물의 전달을 통해 섬유화 부작용의 억제 가능성을 최초로 검증하였다. 특이적으로 모든 그룹에서 대식세포의 수는 동일한 경향성을 보였는데, 이는 대식세포의 표현형에 따른 차이로 검증하였으며, PLGA_MON_SI 그룹의 경우 이식 초기 발생 가능한 M1 표현형의 대식세포가 상대적으로 적게 발현되고, 후기 M2 표현형의 수가 상대적으로 비율이 높게 관찰됨에 따라 생체 내 발생 가능한 면역 반응에 대한 단계적 활성을 조기 종결 시키는 것으로 예측 하였다.

본 연구에서는 위 결과를 바탕으로 몬테루카스트가 실리콘 보형물에 도입되고, 실리콘 보형물에 의해 발생 가능한 섬유화 단계를 다양한 인자들을 통해 조절함으로써 효과적인 섬유화 억제 효과를 구현하였음을 검증하였다. 또한, 초기 섬유화 발생 단계에서의 M2 표현형의 대식세포를 이른 시기에 유도함으로써 섬유화 초기 단계에서의 면역 활성의 조절이 가능함을 검증하였다. 실리콘 보형물의 섬유화 발생 기작에 몬테루카스트 약물을 최초로 적용함으로써, 앞으로 섬유화 발생에 대한 억제 약물로써 의 가능성을 제시하였다.

주요어 : 구형 구축, 몬테루카스트, 섬유화, 실리콘 유방 보형물, 이물반응, 대식세포
표현형

학 번 : 2013-21721